Supporting Information:

Z-Selective Dimerization of Terminal Alkynes by a (PNNP)Fe^{II} Complex

Jeremiah E. Stevens, Justin D. Miller, Matthew C. Fitzsimmons, Curtis E. Moore, and Christine M. Thomas*

Department of Chemistry and Biochemistry, The Ohio State University, Columbus, OH 43210

E-mail: thomasc@chemistry.ohio-state.edu

Contents

1 Experimental Details

1.1 General Considerations

Unless otherwise noted, all manipulations were carried out under an inert atmosphere using a nitrogen- or argon-filled glovebox or standard Schlenk techniques. Glassware was oven-dried before use. Solvents were degassed by sparging with ultra-high purity argon and dried via passage through columns of drying agents using a Glass Contours solvent purification system from Pure Process Technologies. Benzene-d_6 was degassed via repeated freeze-pump-thaw cycles and dried over 3 Å molecular sieves before use. (PNNP)Fe[S1] (**1**) and phenylacetylene-d_1[S2] were prepared according to literature procedures. Phenylacetylene, 4-(trifluoromethyl)phenylacetylene, 4-(*tert*-butyl)phenylacetylene, *p*-tolylacetylene, 4-fluorophenylacetylene, *tert*-butylacetylene, trimethylsilylacetylene, 1-octyne, propargyl alcohol, and *tert*-butylisocyanide were purchased from Sigma Aldrich, dried over $MgSO_4$, purified by vacuum distillation, and stored over 3 Å molecular sieves prior to use. Solid 4-bromophenylacetylene and 4-aminophenylacetylene were purchased from Sigma Aldrich, purified by vacuum sublimation, and dried under mild vacuum for 72 h prior to use. NMR spectra were recorded at ambient temperature unless otherwise stated on a Bruker AVIII 400 MHz or Bruker Avance Neo 400 MHz (with an H-F Prodigy cryoprobe) spectrometer. ^{1}H and ^{13}C{^{1}H} NMR chemical shifts were referenced to residual solvent resonances and are reported in ppm. ^{31}P{^{1}H} NMR chemical shifts (in ppm) were referenced to 85% H_3PO_4 (0 ppm) using an external standard. Solid-state attenuated total reflection infrared spectra (ATR-IR) were acquired using a Bruker Alpha II instrument. Elemental microanalyses were performed by Midwest Microlab, Indianapolis, IN.

1.2 Synthesis of [(PN^{H}N^{H}P)Fe(CCPh)$_2$] (2)

Neat phenylacetylene (0.0160 g, 0.157 mmol, 2.1 equiv) was added by mass to a shell vial, diluted with 1 mL THF, and added dropwise to a 20 mL scintillation vial with a stirring solution of **1** (0.0473 g, 0.0745 mmol) in THF (4 mL). The reaction was allowed to stir for 3 hours, during which the solution changed from a dark red-brown to a deep orange color. After stirring, Et_2O (15 mL) was added, and the mixture was passed through a medium porosity fritted glass funnel. The volatile components were removed from the filtrate in vacuo. The resulting orange-brown residue was washed with pentane (3 $\times$ 3 mL) to remove residual organics and collected on a pipet filter constructed with glass microfiber filter paper. The collected solids were extracted through the filter paper with C_6H_5F (3 mL). A preparative recrystallization was performed by vapor diffusion of methyl *tert*-butyl ether into this concentrated solution of **2** in C_6H_5F at –35 °C. The resulting crystals were collected on a frit to yield spectroscopically pure **2** (0.0225 g, 36.0%). Single crystals

suitable for X-ray diffraction analyses were also obtained using this method. ^{1}H NMR (400 MHz, C_6D_6): δ 7.76 (m, 4H, Ar–H), 7.57 (m, 2H, Ar–H), 7.46 (m, 4H, Ar–H), 7.13–6.75 (overlapping multiplets, 26H, Ar–H), 6.84 (d, J = 8.4 Hz, 2H, Ar–H), 5.80 (d, J = 9.0 Hz, 2H, N–H), 3.09 (dd, J = 10.0 Hz, 7.0 Hz, 2H, CH_2CH_2), 2.61 (m, 2H, CH_2CH_2). ^{31}P{^{1}H} NMR (243 MHz, C_6D_6): δ 76.62 (s, 2P). ^{13}C{^{1}H} NMR (101 MHz, C_6D_6): δ 141.43, 139.19, 137.14, 134.13 (d, J = 17.8 Hz), 131.81, 131.05, 129.23, 128.89, 128.78, 128.66 (d, J = 9.8 Hz), 124.05, 123.59, 117.95, 110.83, 107.75, 96.48 (C≡C), 89.00 (C≡C), 43.30. ATR-IR (cm^{-1}): 2046 (C≡C), 3021 (N−H). Due to the extreme air and moisture sensitivity of this compound, elemental microanalysis failed to provide acceptable results.

1.3 Synthesis of [(PNNP)Fe(CN^{t}Bu)$_2$] (3)

To a 20mL scintillation vial equipped with a stir bar, **1** (12.2 mg, 0.0192 mmol) was dissolved in 2 mL of C_6H_6. CN^{t}Bu (4.78 µL, 2.2 equiv) was added via micropipet. The mixture was stirred for 10 minutes, during which the color changed from the deep red/brown of **1** to a very intense bright orange. The volatile components were removed from the mixture in vacuo via lyophilization to yield an analytically pure yellow-orange powder (15.1 mg, 0.0189 mmol, 98%). Single crystals suitable for X-ray diffraction analyses were grown by slow evaporation of an Et_2O solution of **3** at –35 °C. ^{1}H NMR (400 MHz, C_6D_6): δ 7.56 (t, J = 8.1 Hz, 8H, Ar–H), 7.23 (m, 4H, Ar–H), 6.99 (m, 14H, Ar–H), 6.39 (t, J = 7.3, 2H, Ar–H), 3.56 (s, 4H, CH_2CH_2), 0.55 (s, 18H, $(CH_3)_3$). ^{31}P{^{1}H} NMR (162 MHz, C_6D_6): δ 70.04 (s, 2P, PPh_2). ^{13}C{^{1}H} NMR (101 MHz, C_6D_6): 168.47 (m), 167.31, 140.16 (m), 134.18, 133.72 (t, J = 5.1 Hz), 131.41, 128.59, 119.94 (m), 112.76 (t, J = 6.0 Hz), 108.82 (t, J = 3.5 Hz), 55.65, 54.09, 30.17. ATR-IR (cm^{-1}): 2111 (C≡N). Anal. Calcd. for $C_{48}H_{50}FeN_4P_2$: 72.00 % C, 6.29% H, 7.00% N; Found: 71.80% C, 6.13% H, 5.74% N.

1.4 General procedure for catalytic runs

To a stirring solution of **1** in C_6D_6 (approximately 0.7 mL), the alkyne substrate was added by mass to the solution. The mixture was then capped, placed on a stirring hotplate set at 30 °C, and allowed to stir for 2 hours. Following this, a stock solution of an appropriate internal integral standard (hexamethylbenzene for most; trimethoxybenzene for substrates with *para*-substituted alkyl groups) was added for purposes of quantification, and the product yield and substrate conversions were determined with quantitative ^{1}H NMR spectroscopy. Due to longer T_1 relaxation times of the alkenyl signals expected in the absence of O_2, the relaxation delay time (`d1`) was set to 45 seconds. Quantified NMR spectra are presented in Figures S29–S34.

1.5 Dimerization of 4a

Following the general procedure outlined in Section 1.4, **1** (79.9 mg of solution, 0.00268 mmol) was added a stock solution (0.0335 mmol **1**/ g soln.) in C_6D_6 to a vial containing a stir bar and approximately 0.7 mL C_6D_6. To this, **4a** (26.1 mg, 0.255 mmol, 95 equiv) was added by mass. Upon completion of the reaction, the integral standard hexamethylbenzene (137.5 mg of solution, 0.127 mmol, 47.5 equiv) in C_6D_6 (0.928 mmol HMB / g soln.). ^{1}H NMR of *Z*-dimer (400 MHz, C_6D_6): δ 7.93 (d, J = 7.3 Hz, 2H, Ar–H), 7.44 (d, J = 8.0 Hz, 2H, Ar–H), 7.01 (overlapping m, 6H, Ar–H), 6.41 (d, J = 12.0 Hz, 1H, C=C–H), 5.80 (d, J = 11.9 Hz, 1H, C=C–H). Olefinic C – H of *E*-dimer: 6.30 (d, J = 16.3 Hz). The second doublet of the *E*-dimer was obscured by the aromatic region. Product formation was verified by comparison of the ^{1}H NMR spectrum to literature data.[S3]

1.6 Dimerization of 4b

Following the general procedure outlined in Section 1.4, **1** (22.1 mg of solution, 0.00332 mmol) was added a stock solution (0.150 mmol **1**/ g soln.) in C_6D_6 to a vial containing a stir bar and approximately 0.7 mL C_6D_6. To this, **4b** (49.8 mg, 0.314 mmol, 95 equiv) was added by mass. Upon completion of the reaction, the integral standard 1,3,5-trimethoxybenzene (145.5 mg of solution, 0.0975 mmol, 29.5 equiv) in C_6D_6 (0.670 mmol TMB / g soln.). ^{1}H NMR of *Z*-dimer (400 MHz, C_6D_6): δ 8.02 (d, J = 8.5 Hz, 2H, Ar–H), 7.51 (d,J = 8.4 Hz, 2H, Ar–H), 7.33 (d, J = 8.5 Hz, 2H, Ar–H), 7.12 (d, J = 8.4 Hz, 2H, Ar–H), 6.50 (d, J = 11.9 Hz, 1H, C=C–H), 5.87 (d, J = 11.9 Hz, 1H, C=C–H), 1.21 (s, 9H, ^{t}Bu), 1.13 (s, 9H, ^{t}Bu). Olefinic C – H of *E*-dimer: 6.42 (d, J = 16.3 Hz). The second doublet of the *E*-dimer was obscured by the aromatic region. Product formation was verified by comparison of the ^{1}H NMR spectrum to literature data.[S4]

1.7 Dimerization of 4c

Following the general procedure outlined in Section 1.4, **1** (84.7 mg of solution, 0.00284 mmol) was added a stock solution (0.0335 mmol **1**/ g soln.) in C_6D_6 to a vial containing a stir bar and approximately 0.7 mL C_6D_6. To this, **4c** (32.5 mg, 0.271 mmol, 95 equiv) was added by mass. Upon completion of the reaction, the integral standard hexamethylbenzene (145.2 mg of solution, 0.135 mmol, 47.5 equiv) in C_6D_6 (0.928 mmol HMB / g soln.). ^{1}H NMR of *Z*-dimer (400 MHz, C_6D_6): δ 7.67 (m, 2H, Ar–H), 7.14 (m, 2H, Ar–H), 6.78 (t, J = 8.8 Hz, 2H, Ar–H), 6.60 (t, J = 8.8 Hz, 2H, Ar–H), 6.26 (d, J = 11.9 Hz, 1H, C=C–H), 5.70 (d, J = 12.0 Hz, 1H, Ar–H). Olefinic C – H of *E*-dimer: 6.09 (d, J = 16.3 Hz). The second doublet of the *E*-dimer was obscured by the aromatic region. Product formation was verified by comparison of the ^{1}H NMR spectrum to literature data.[S4]

1.8 Dimerization of 4d

Following the general procedure outlined in Section 1.4, **1** (33.6 mg of solution, 0.00504 mmol) was added a stock solution (0.150 mmol **1**/ g soln.) in C_6D_6 to a vial containing a stir bar and approximately 0.7 mL C_6D_6.To this, **4d** (18.3 mg, 0.102 mmol, 20 equiv) was added by mass. Upon completion of the reaction, the integral standard hexamethylbenzene (18.0 mg of solution, 0.00739 mmol, 1.4 equiv) in C_6D_6 (0.410 mmol HMB / g soln.). ^{1}H NMR of *Z*-dimer (400 MHz, C_6D_6): δ 7.49 (d, J = 8.6 Hz, 2H, Ar–H), 7.41 (d, J = 8.0 Hz, 2H, Ar–H), 7.25 (d, J = 8.6 Hz, 2H, Ar–H), 7.08 (d, J = 8.5 Hz, 2H, Ar–H), 6.19 (d, J = 11.9 Hz, 1H, C=C–H), 5.68 (d, J = 11.9 Hz, 1H, C=C–H). Olefinic C – H of *E*-dimer: 6.08 (d, J = 16.3 Hz). The second doublet of the *E*-dimer was obscured by the aromatic region. Product formation was verified by comparison of the ^{1}H NMR spectrum to literature data.[S3]

1.9 Dimerization of 4e

Following the general procedure outlined in Section 1.4, **1** (80.0 mg of solution, 0.00268 mmol) was added a stock solution (0.0335 mmol **1**/ g soln.) in C_6D_6 to a vial containing a stir bar and approximately 0.7 mL C_6D_6. To this, **4e** (43.3 mg, 0.255 mmol, 95 equiv) was added by mass. Upon completion of the reaction, the integral standard hexamethylbenzene (137.2 mg of solution, 0.127 mmol, 47.5 equiv) in C_6D_6 (0.928 mmol HMB / g soln.). ^{1}H NMR of *Z*-dimer (400 MHz, C_6D_6): δ 7.64 (d, J = 8.1 Hz, 2H, Ar–H), 7.01 (m, 2H, Ar–H), 6.25 (d, J = 11.9 Hz, 1H, C=C–H), 5.73 (d, J = 12.0 Hz, 1H, C=C–H). Remaining two Ar–H signals (4 H total) could not be located due to their overlap with aromatic peaks corresponding to unreacted alkyne. Olefinic C – H of *E*-dimer: 6.12 (d, J = 16.3 Hz). The second doublet of the *E*-dimer was obscured by the aromatic region. Product formation was verified by comparison of the ^{1}H NMR spectrum to literature data.[S4]

1.10 Dimerization of 4f

Following the general procedure outlined in Section 1.4, **1** (30.5 mg of solution, 0.00457 mmol) was added a stock solution (0.150 mmol **1**/ g soln.) in C_6D_6 to a vial containing a stir bar and approximately 0.7 mL C_6D_6.To this, **4f** (10.7 mg, 0.0914 mmol, 20 equiv) was added by mass. Upon completion of the reaction, the integral standard hexamethylbenzene (19.5 mg of solution, 0.00800 mmol, 1.8 equiv) in C_6D_6 (0.410 mmol HMB / g soln.). ^{1}H NMR of *Z*-dimer (400 MHz, C_6D_6): δ 6.29 (d, J = 12.0 Hz, 1H, C=C–H), 5.75 (d, J = 11.9 Hz, 1H, C=C–H). The four Ar–H signals (8 H total) and two NH_2 signals (4 H total) could not be located due to the low yield of this product. The *E*-dimer was not detected for this substrate.

1.11 Catalytic Investigation of 2

In a 20 mL scintillation vial equipped with a stir bar, **2** (19.1 mg, 0.023 mmol) was dissolved in C_6H_6 (1 mL). Neat phenylacetylene (260 µL, 2.3 mmol, 100 equiv) was added by micropipet. The vial was then stirred on a hot plate at 30 °C for 1 h. Following this, the volatile components were removed in vacuo to analyze the resulting product mixture and confirm that the organic dimer had been formed.

1.12 Preparation of [(PN^{D}N^{D}P)Fe(CCPh)$_2$] (2-D) and PhCCH Crossover Experiment

Following the synthesis described for **2** in Section 1.2, neat phenylacetylene-d_1 (0.0219 g, 0.214 mmol, 2.2 equiv) was added by mass to a shell vial, diluted with 1 mL THF, and added dropwise to a 20 mL scintillation vial containing a stirring solution of **1** (0.0619 g, 0.0976 mmol) in THF (4 mL). The reaction was allowed to stir for 3 hours, during which the solution changed from a dark red-brown to a deep orange color. After stirring, Et_2O (15 mL) was added, and the mixture was passed through a medium porosity fritted glass funnel. The volatile components were removed from the filtrate in vacuo. The resulting orange-brown residue was washed with pentane (3 × 3 mL) to remove residual organics and collected on a pipet filter constructed with glass microfiber filter paper. The collected solids were extracted through the filter paper with C_6H_5F (3 mL). A preparative recrystallization was performed by vapor diffusion of methyl *tert*-butyl ether into this concentrated solution of **2-D** in C_6H_5F at –35°C. These crystals were collected on a frit to yield spectroscopically pure **2-D** (0.0288 g, 0.0343 mmol, 35.1%). ^{1}H NMR (400 MHz, C_6D_6, Figure S42): δ 7.76 (m, 4H, Ar–H), 7.57 (m, 2H, Ar–H), 7.46 (m, 4H, Ar–H), 7.11–6.83 (overlapping multiplets, 28H, Ar–H), 3.09 (apparent t, J = 8.9 2H, CH_2CH_2), 2.60 (m, 2H, CH_2CH_2). This NMR spectrum is consistent with that of **2**, except the N–H resonance is missing in **2-D**.

The entire quantity of **2-D** (0.0288 g, 0.0343 mmol) was then added to a 20 mL scintillation vial equipped with a stir bar and dissolved in THF (3 mL). To this stirring solution, phenylacetylene (15.2 µL, 0.14 mmol, 4.0 equiv) was added and allowed to stir for 3 h, during which time no color change was noted. Following this, the product was precipitated using cold (–35 °C) Et_2O and collected on a filter pipet constructed with glass microfiber filter paper. The product was the extracted from the filter pipet using THF, and volatile components were removed in vacuo. The resulting residue was dissolved in C_6D_6 for ^{1}H NMR analysis (Figure S42). Following this, the NMR sample of the metal complex was recombined with the extracted organic material in Et_2O from above and stripped of the metal complex by passage through a silica plug with 3 mL of C_6H_6 as an eluent, and volatiles were removed from the isolated organic product in vacuo. The yellow-white residue was dissolved in 0.75 mL of C_6H_6, and 2 drops of C_6D_6 were added to this solution before transferring to a fresh NMR tube for ^{2}H NMR analysis (Figure S43).

1.13 ^{57}Fe Mössbauer Spectroscopy Details

Samples for ^{57}Fe Mössbauer spectroscopy were prepared by suspending approximately 30 mg of sample in Paratone®-N cryoprotectant oil and loaded into the sample holder under liquid N_2. Spectra were obtained at $\leqslant$4 K over a 24-hour period using a See Co. (Minneapolis, MN) constant-acceleration spectrometer equipped with a Janis SHI-4 cryostat. Isomer shifts (δ) are reported relative to a 25-μm thick sample of α-Fe foil at 295 K. Data folding and fitting routines were performed using the WMOSS-4F software package.[S5]

2 Crystallographic Details

2.1 Collection, Solution, and Refinement of 2

The single crystal X-ray diffraction studies were carried out on a Bruker D8 Venture Kappa diffractometer equipped with Mo(TXS-HB) K_α radiation (λ = 0.71073 Å) and a Photon III CPAD detector. The crystal was mounted on a MiTeGen Micromount with Paratone 24EX oil. Data were collected in a nitrogen gas stream at 100(2) K using ϕ and ω scans. Data collection was 99.9% complete to 25° in θ (0.83 Å). The crystal-to-detector distance was 60 mm using variable exposure time (4 s to 10 s) depending on θ with a scan width of 1.0°. A total of 152 619 reflections were collected with $-36 \leqslant h \leqslant 36$, $-17 \leqslant k \leqslant 17$, $-20 \leqslant l \leqslant 20$. Of these, 6325 reflections were found to be symmetry independent, with a R_{int} of 0.0627. Indexing and unit cell refinement indicated a C-centered monoclinic lattice with space group C2/c. The data were integrated using the Bruker SAINT[S6] software program and scaled using the SADABS[S7] software program. Structure solution and refinement were done within the Olex2 software package.[S8] Solution by direct methods (SHELXT[S9]) produced a complete phasing model for refinement. All nonhydrogen atoms were refined anisotropically by full-matrix least-squares (SHELXL-2014[S10]). All carbon-bonded hydrogen atoms were placed using a riding model with positions constrained relative to their parent atom using the appropriate HFIX command in SHELXL-2014. The nitrogen-bonded hydrogens were located in the difference map, and their relative positions and thermal parameters were freely refined. A summary of determined parameters and refinement statistics are available in Table S1.

2.2 Collection, Solution, and Refinement of 3

The single crystal X-ray diffraction studies were carried out on a Bruker D8 Venture Kappa diffractometer equipped with Mo(TXS-HB) K_α radiation (λ = 0.71073 Å) and a Photon III CPAD detector. The crystal was mounted on a MiTeGen Micromount with Paratone 24EX oil. Data were collected in a nitrogen gas stream at

100(2) K using ϕ and ω scans. Data collection was 99.9% complete to 25° in θ (0.83 Å). The crystal-to-detector distance was 50 mm using variable exposure time (2 s to 10 s) depending on θ with a scan width of 1.0°. A total of 101 157 reflections were collected with $-13 \leqslant h \leqslant 13$, $-17 \leqslant k \leqslant 17$, $-18 \leqslant l \leqslant 18$. Of these, 8545 reflections were found to be symmetry independent, with a R_{int} of 0.0489. Indexing and unit cell refinement indicated a primitive triclinic lattice with space group $P\bar{1}$. The data were integrated using the Bruker SAINT[S6] software program and scaled using the SADABS[S7] software program. Structure solution and refinement were done within the Olex2 software package.[S8] Solution by direct methods (SHELXT[S9]) produced a complete phasing model for refinement. All nonhydrogen atoms were refined anisotropically by full-matrix least-squares (SHELXL-2014[S10]). All hydrogen atoms were placed using a riding model with positions constrained relative to their parent atom using the appropriate HFIX command in SHELXL-2014. A summary of determined parameters and refinement statistics are available in Table S1.

2.3 Collection, Solution, and Refinement of 5 + 6

The single crystal X-ray diffraction studies were carried out on a Bruker D8 Venture Kappa diffractometer equipped with Mo(TXS-HB) K_α radiation (λ = 0.71073 Å) and a Photon III CPAD detector. The crystal was mounted on a MiTeGen Micromount with Paratone 24EX oil. Data were collected in a nitrogen gas stream at 100(2) K using ϕ and ω scans. Data collection was 99.9% complete to 25° in θ (0.83 Å). The crystal-to-detector distance was 50 mm using variable exposure time (2 s to 10 s) depending on θ with a scan width of 1.0°. A total of 127 110 reflections were collected with $-16 \leqslant h \leqslant 16$, $-17 \leqslant k \leqslant 17$, $-18 \leqslant l \leqslant 18$. Of these, 10 359 reflections were found to be symmetry independent, with a R_{int} of 0.0676. Indexing and unit cell refinement indicated a primitive triclinic lattice with space group $P\bar{1}$. The data were integrated using the Bruker SAINT[S6] software program and scaled using the SADABS[S7] software program. Structure solution and refinement were done within the Olex2 software package.[S8] Solution by direct methods (SHELXT[S9]) produced a complete phasing model for refinement. All nonhydrogen atoms were refined anisotropically by full-matrix least-squares (SHELXL-2014[S10]). All hydrogen atoms were placed using a riding model with positions constrained relative to their parent atom using the appropriate HFIX command in SHELXL-2014. The final solution shows **5** as the major component with an occupancy of 75% and **6** as the minor component with an occupancy of 25%. A summary of determined parameters and refinement statistics are available in Table S1.

2.4 Collection, Solution, and Refinement of 7

The single crystal X-ray diffraction studies were carried out on a Bruker D8 Venture Kappa diffractometer equipped with Mo(TXS-HB) K_α radiation (λ = 0.71073 Å) and a Photon III CPAD detector. The crystal was mounted on a MiTeGen Micromount with Paratone 24EX oil. Data were collected in a nitrogen gas stream at 100(2) K using ϕ and ω scans. Data collection was 99.9% complete to 25° in θ (0.83 Å). The crystal-to-detector distance was 50 mm using variable exposure time (2 s to 10 s) depending on θ with a scan width of 1.0°. A total of 106 352 reflections were collected with $-14 \leqslant h \leqslant 14$, $-15 \leqslant k \leqslant 15$, $-21 \leqslant l \leqslant 21$. Of these, 8759 reflections were found to be symmetry independent, with a R_{int} of 0.0554. Indexing and unit cell refinement indicated a primitive triclinic lattice with space group $P\bar{1}$. The data were integrated using the Bruker SAINT[S6] software program and scaled using the SADABS[S7] software program. Structure solution and refinement were done within the Olex2 software package.[S8] Solution by direct methods (SHELXT[S9]) produced a complete phasing model for refinement. All nonhydrogen atoms were refined anisotropically by full-matrix least-squares (SHELXL-2014[S10]). The **4e**-derived terminal H (labeled H1 in Figure S17) was located in the difference map, and its position and ADPs were freely refined. All other hydrogen atoms were placed using a riding model with positions constrained relative to their parent atom using the appropriate HFIX command in SHELXL-2014. A summary of determined parameters and refinement statistics are available in Table S1.

3 Discussion of the Metal Complexes Obtained in Catalytic and/or Stoichiometric Reactions between 1 and 4a–4e

During the catalytic runs with **4e** and, to a lesser extent, **4c** (Figure S2), we discovered that an appreciable quantity of an asymmetric metal complex is formed in addition to a structural analogue of **2**. To probe this formation, we treated **1** (25.6 mg, 0.040 mmol) with 2.2 equiv **4e** (15.0 µL, 0.092 mmol) in THF at –78 °C for 90 min. The $^{31}P\{^1H\}$ NMR spectrum of the reaction mixture after 2 h (Figure S3) exhibits a pair of doublets integrating 1:1 to each other and a singlet integrating to 2 relative to one of the doublets. We attribute the singlet to the aforementioned bis(acetylide) complex **5** analogous to **2**, whereas the pair of doublets corresponds to a new asymmetric product **6** with inequivalent phosphine donors. On the basis of this $^{31}P\{^1H\}$ spectrum, the asymmetric complex is formed in a 2:1 ratio with respect to the bis(acetylide) complex.

The $^{19}F\{^1H\}$ spectrum (Figure S4) exhibits three singlets attributable to metal-containing species that integrate 1:1:1 relative to each other. Based on the 2:1 relative integration of the asymmetric species to

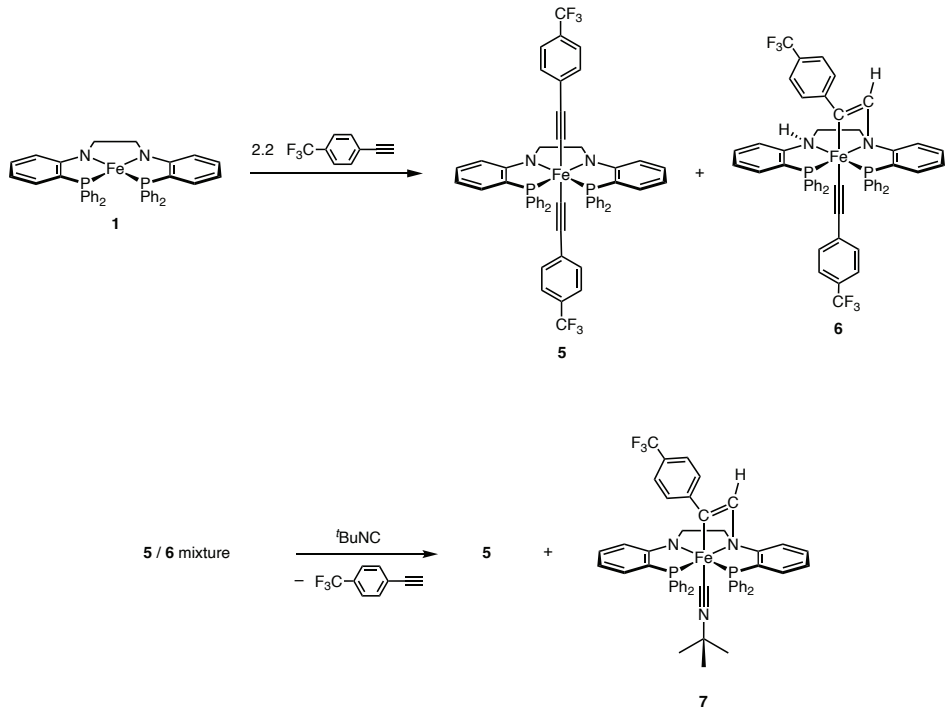

Figure S1: Reaction of **1** with 2 equiv **4e** to form the **5** + **6** mixture (top) and derivatization of **6** by treatment of the mixture with 1 equiv CN^{t}Bu (bottom). A detailed discussion of these complexes follows in-text.

the bis(acetylide) complex and the observed symmetries of these complexes, one of these singlets (–61.3 ppm, determined by comparison to the spectrum in Figure S9) corresponds to the 6 equivalent fluorine atoms of the two CF_3 groups of the symmetric bis(acetylide) complex **5**, whereas the other two singlets each correspond to three fluorine atoms of two chemically inequivalent CF_3 environments of the asymmetric complex **6**.

The ^{1}H NMR spectrum (Figure S5) of this mixture contains a broad doublet at 5.58 ppm integrating to 2, corresponding to the two amine protons of the bis(phenylacetylide) complex **5**. On the basis of a ^{1}H COSY experiment (Figure S7), the resonance at 2.95 corresponds to one pair of ethylene backbone protons on the bis(acetylide), and the other resonance for the second pair of backbone protons is overlapping with peaks for the asymmetric species at approximately 2.64 ppm. The asymmetric species **6** has 4 ethylene backbone resonances that appear as multiplets at 3.39 and 3.20, with two more multiplets overlapping with the aforementioned backbone resonance of the bis(acetylide) complex at approximately 2.64 ppm. The ethylene backbone protons of **6** integrate 1:1 relative to each other and with a combined integration consistent with a 2:1 ratio of **6** to **5**. The presence of distinct resonances for each backbone proton in **6** suggests a break of both the horizontal and vertical mirror planes of the (PNNP)Fe complex.

Interestingly, in the ^{1}H NMR spectrum of the **5**/**6** mixture, there is a doublet of doublets at 5.95 ppm

that corresponds to 1H on **6** due to its 1:1 relative integration to the ethylene backbone resonances of **6**. The chemical shift of this resonance suggests that it is olefinic in nature. Additionally, the resonance in question exhibits coupling in the ^{1}H spectrum (J = 1.51, 3.14, left inset of Figure S5) but not in the ^{1}H{^{31}P} spectrum (right inset of Figure S5), suggesting that this could be $^{4}J_{\text{P–H}}$ coupling to the inequivalent phosphines, which is not uncommon in ^{31}P NMR spectroscopy.[S11] Additionally, a well-resolved doublet (J = 8.28 Hz) centered at 5.27 ppm and integrating to 2H on the asymmetric species (2:1 relative to the ethylene backbone resonances of the asymmetric species) is also present. This doublet is not coupled to the phosphine donors, as it maintains its coupling in the ^{1}H{^{31}P} spectrum, unlike the doublet of doublets centered at 5.95 ppm. This resonance does, however, couple to other aromatic signals in the COSY spectrum (Figure S7), so we attribute this to an upfield-shifted aromatic resonance.

Indeed, single crystals grown from evaporation of a supersaturated Et_2O solution of the above reaction mixture at –35 °C revealed the bis(4-(trifluoromethyl)phenylacetylide) complex **5** (Figure S15) as the major component (75%) with crystallographic disorder that revealed a second, minor component (25%) **6** (Figure S16) wherein the alkyne has undergone a [2+2] cycloaddition with the Fe−N bond. The resulting C−C distance is elongated ($d_{\text{C=C}} = 1.343(16)$ Å) and consistent with a C=C double bond. Due to the small amount of this minor component and complications from disorder, we were unable to locate any of the minor component's H atoms in the difference map. We therefore opted to explore chemical modification as a strategy to affect separation of the mixture of **5** and **6**, as any physical methods of separation were unsuccessful owing to the very similar solubilities of both components.

Addition of 1.0 equiv of CN^{t}Bu (3.62 µL,0.032 mmol) to the **5**/**6** mixture (30.9 mg, 0.032 mmol) in THF and stirring for 30 min results in the displacement of the 4-(trifluoromethyl)-phenylacetylide moiety of **6** (lost as **4e**), leaving behind the alkyne fragment that bridges the Fe−N bond. Complex **5** does not react with CN^{t}Bu and remains unreacted in the mixture. A single crystal of the resulting species **7** was obtained from a co-crystallized mixture of **7** and **5** (Figure S17). Importantly, the **4e**-derived H (H1 in Figure S17) was located in the difference map, and its position and thermal parameters were freely refined. The ^{31}P{^{1}H} NMR spectrum (Figure S8) of the mixture of **5** and **7** reveals that **5** is untouched, whereas the two doublets corresponding to **6** have both shifted positions, consistent with the conversion of **6** to **7**. The ^{19}F{^{1}H} spectrum (Figure S9) also reveals that the singlet for **5** has remained unchanged, but the two singlets previously attributed to **6** are no longer present, leaving behind one new singlet corresponding to the sole CF_3 environment of **7**. Most interestingly, however, is the ^{1}H NMR spectrum (Figure S10), wherein the two resonances in question from the **5**/**6** mixture (in dashed boxes in Figures S5 and S10) are still present in a 1:2 ratio and are now shifted slightly, likely owing to the change in ligand identity *trans* to the Fe−C bond. We

conclude, therefore, that this derivatization experiment confirms our hypothesis that the dd at 5.95 ppm in the ^{1}H spectrum of the **5**/**6** mixture (Figure S5) corresponds to the **4e**-derived terminal olefininc H (H10B in Figure S16), and the doublet at 5.27 ppm (2H) is an upfield-shifted aromatic resonance of **6**.

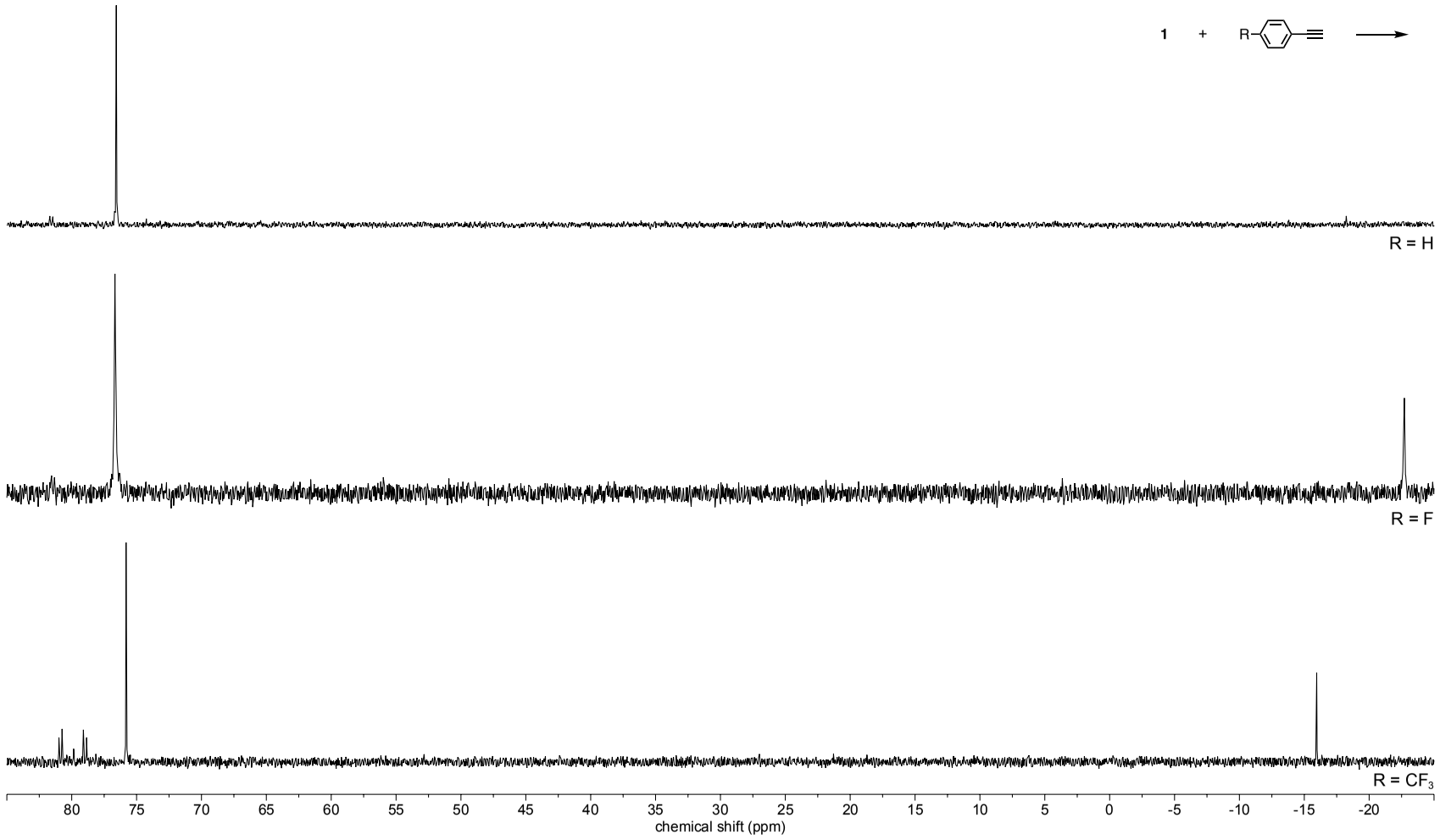

Figure S2: $^{31}P\{^{1}H\}$ NMR spectra (C_6H_6, 101 MHz) of the post-catalytic mixtures resulting from treatment of **1** with 99 equiv. of **4a** (top), **4c** (middle), and **4e** (bottom).

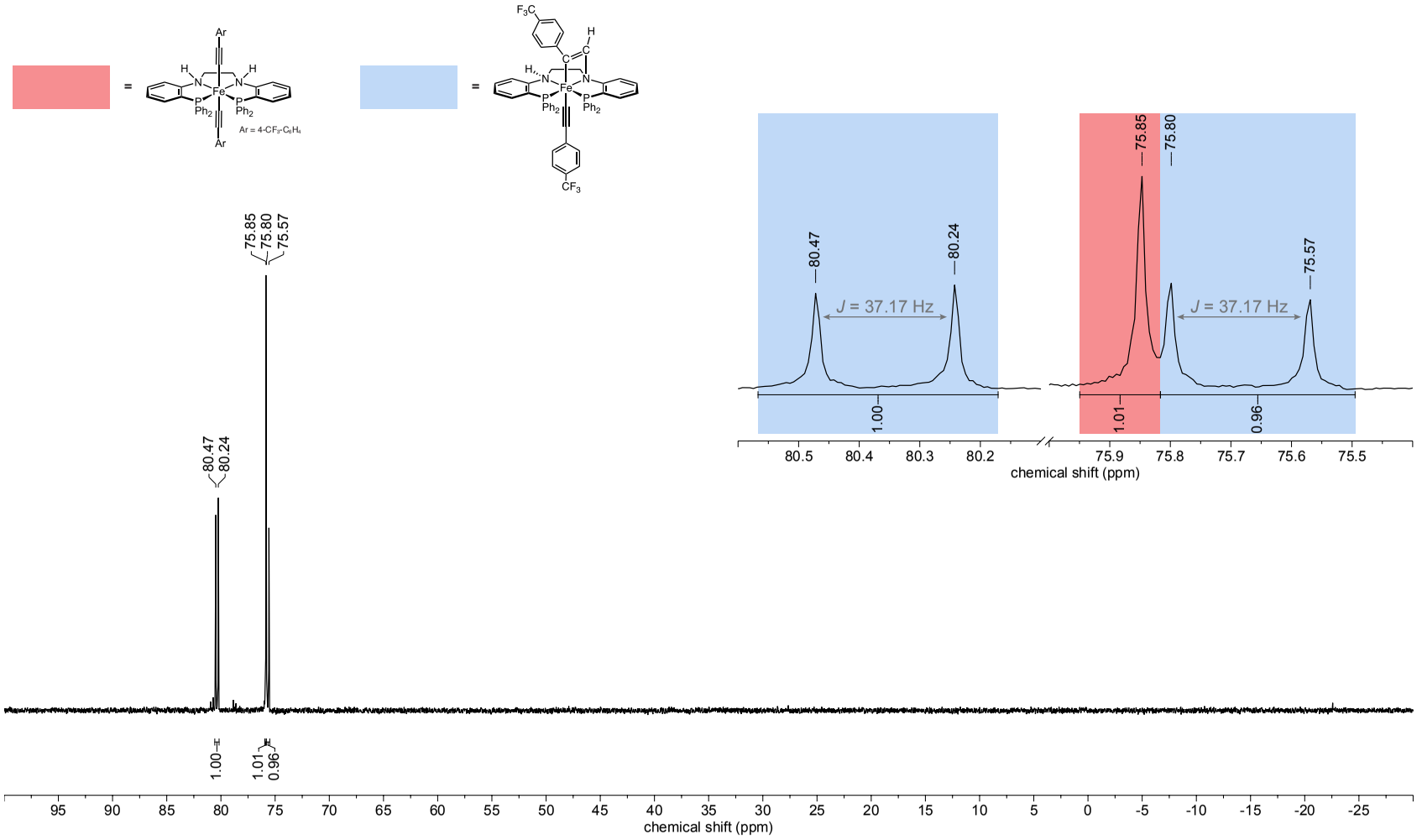

Figure S3: $^{31}P\{^{1}H\}$ NMR spectrum (C_6D_6, 101 MHz) resulting from the treatment of **1** with 2.2 equiv **4e**.

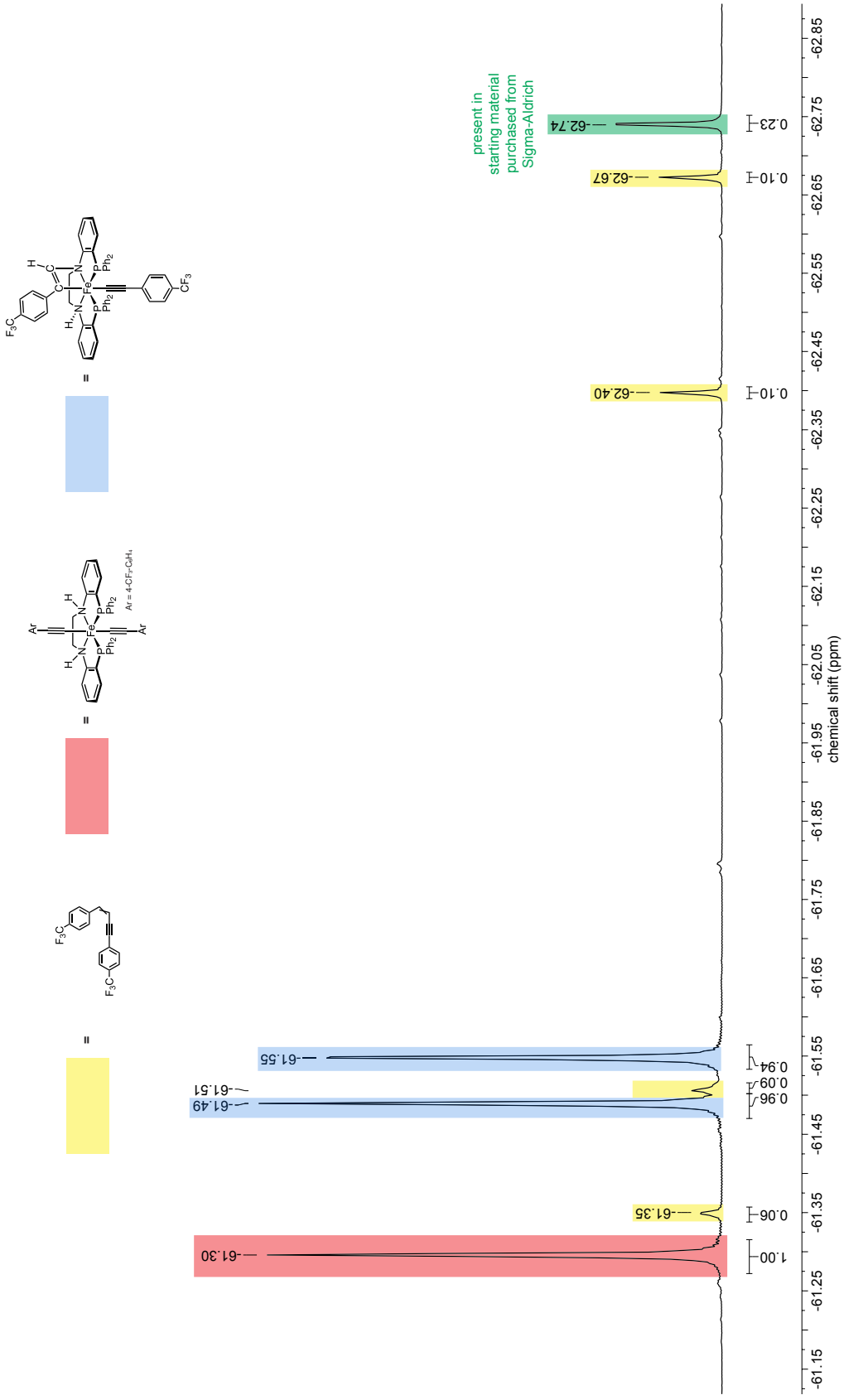

Figure S4: $^{19}F\{^{1}H\}$ spectrum (C_6D_6, 376.5 MHz) resulting from the treatment of **1** with 2.2 equiv **4e**.

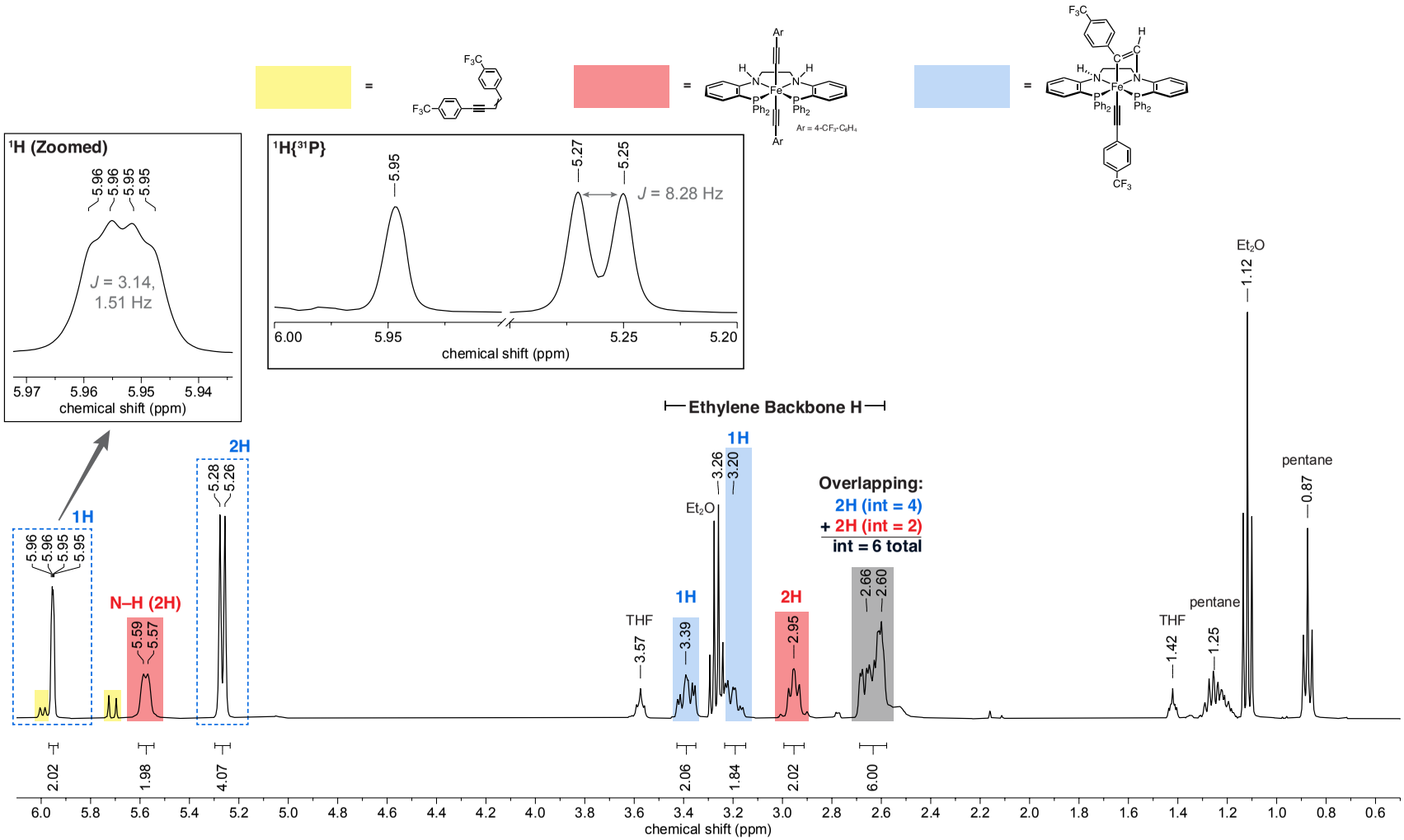

Figure S5: Aliphatic region of the ^{1}H NMR spectrum (C_6D_6, 400 MHz) resulting from the treatment of **1** with 2.2 equiv **4e**. The numbers given in blue/red text by each highlighted resonance refer to the number of H to which each resonance corresponds on the asymmetric and bis(acetylide) complexes, respectively. The two insets show a zoomed-in version of the multiplet at 5.95 ppm in the ^{1}H NMR spectrum (left) and the 6 to 5.2 ppm region of the ^{1}H{^{31}P} NMR spectrum (right).

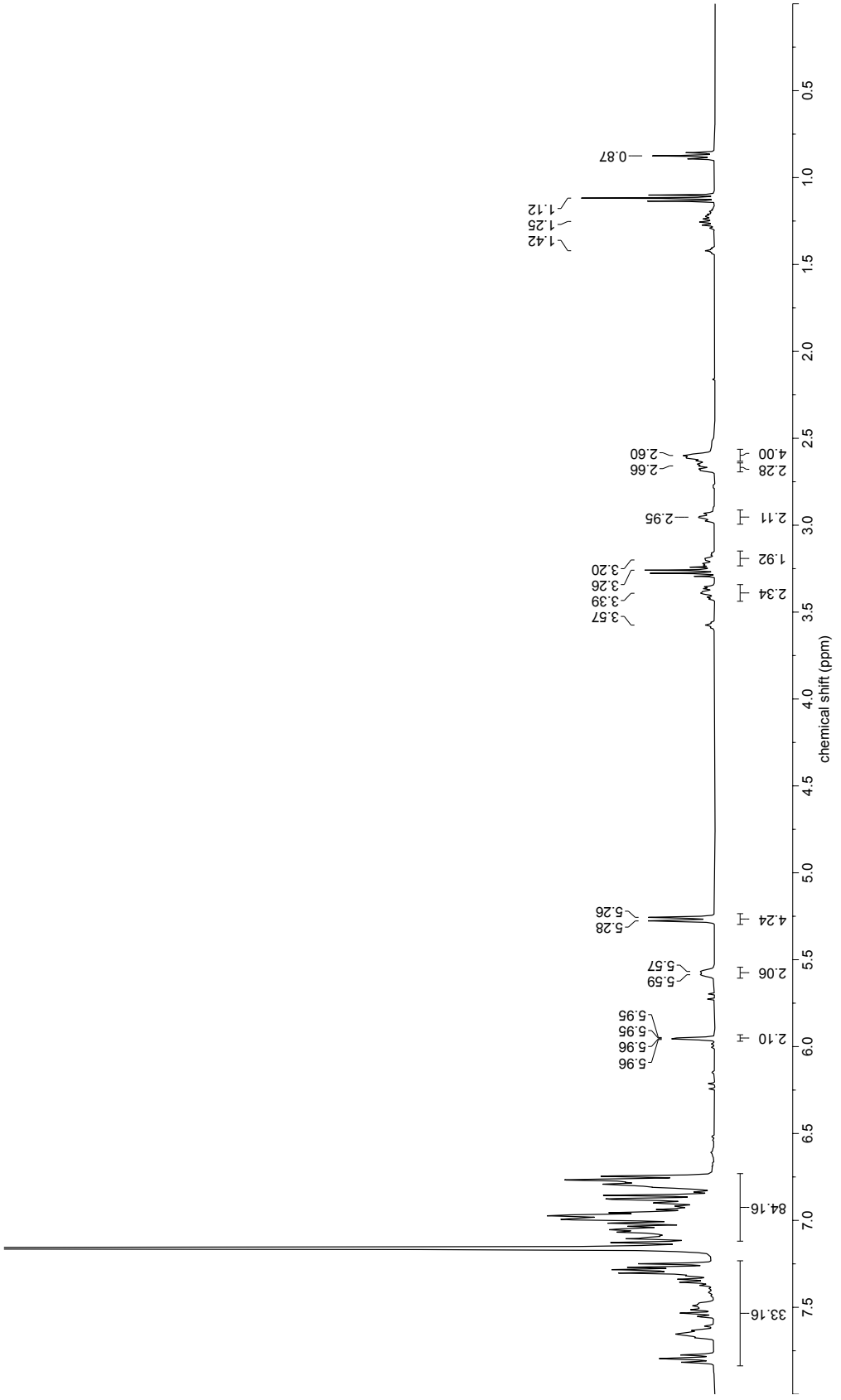

Figure S6: Full ^{1}H NMR spectrum (C_6D_6, 400 MHz) resulting from the treatment of **1** with 2.2 equiv **4e**.

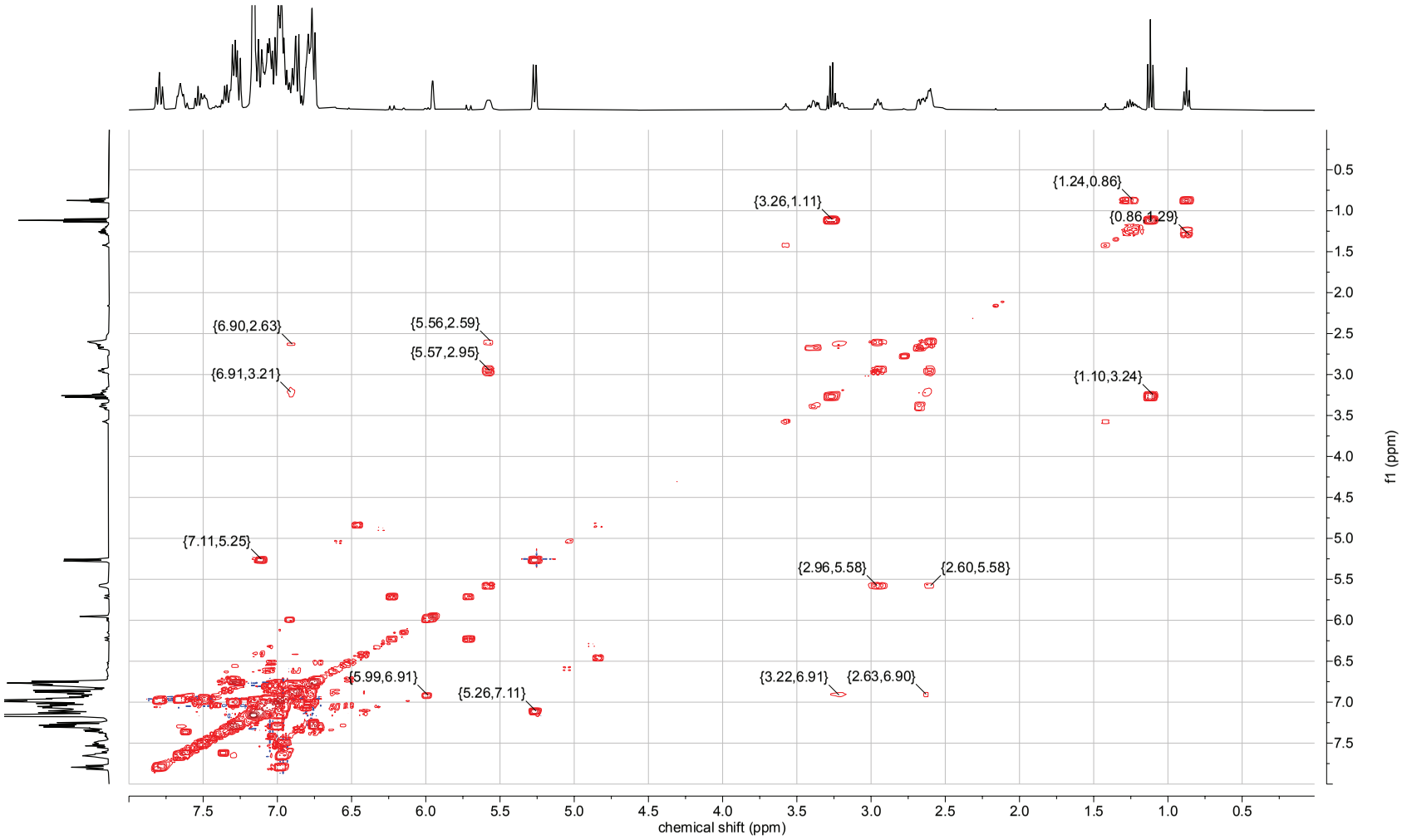

Figure S7: $^{1}H-^{1}H$ COSY (C_6D_6, 400 MHz) resulting from the treatment of **1** with 2.2 equiv **4e** used to assign peaks in Figure S5

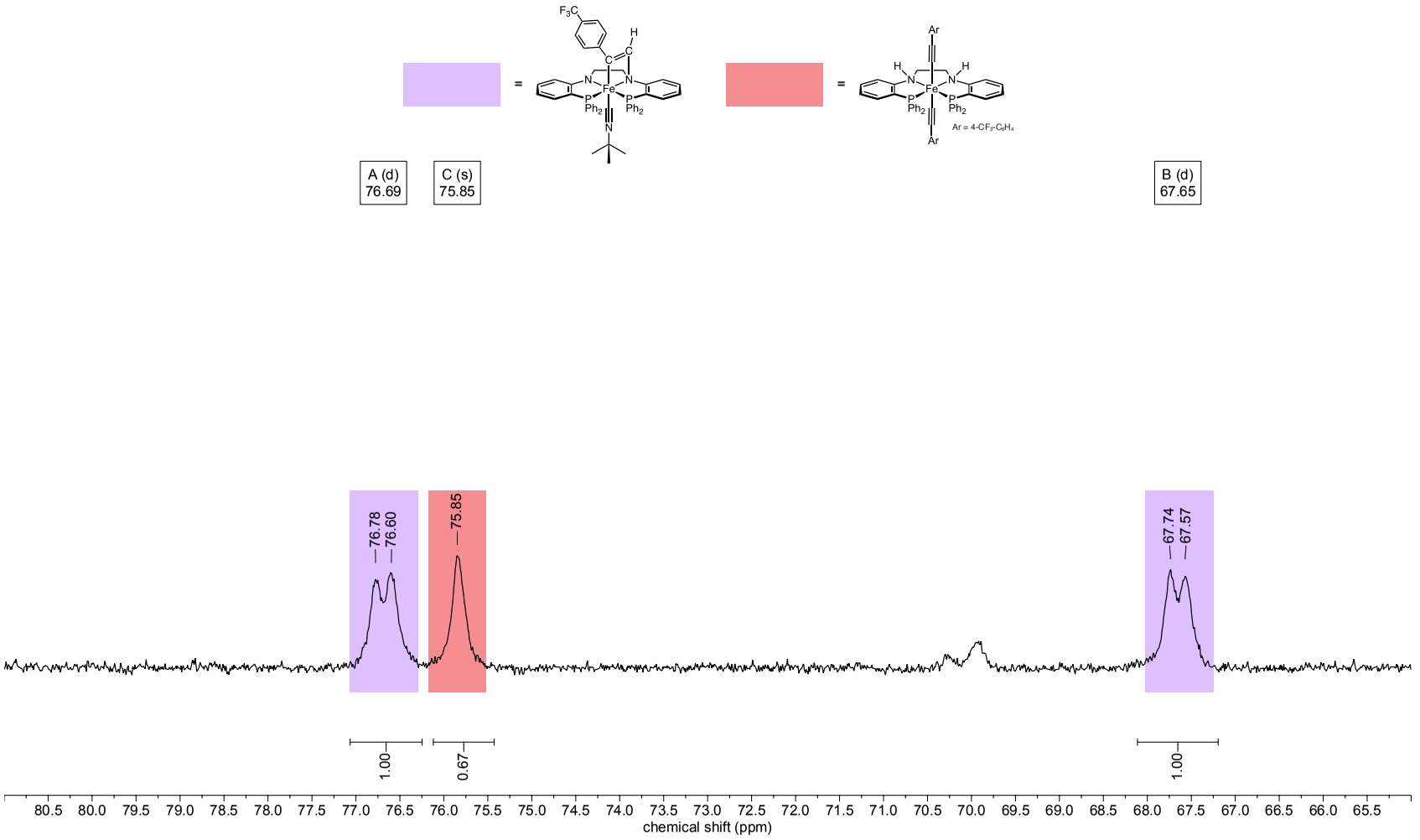

Figure S8: $^{31}P\{^{1}H\}$ NMR spectrum (C_6D_6, 101 MHz) resulting from the treatment of the **5** + **6** mixture with 1.0 equiv CN^tBu.

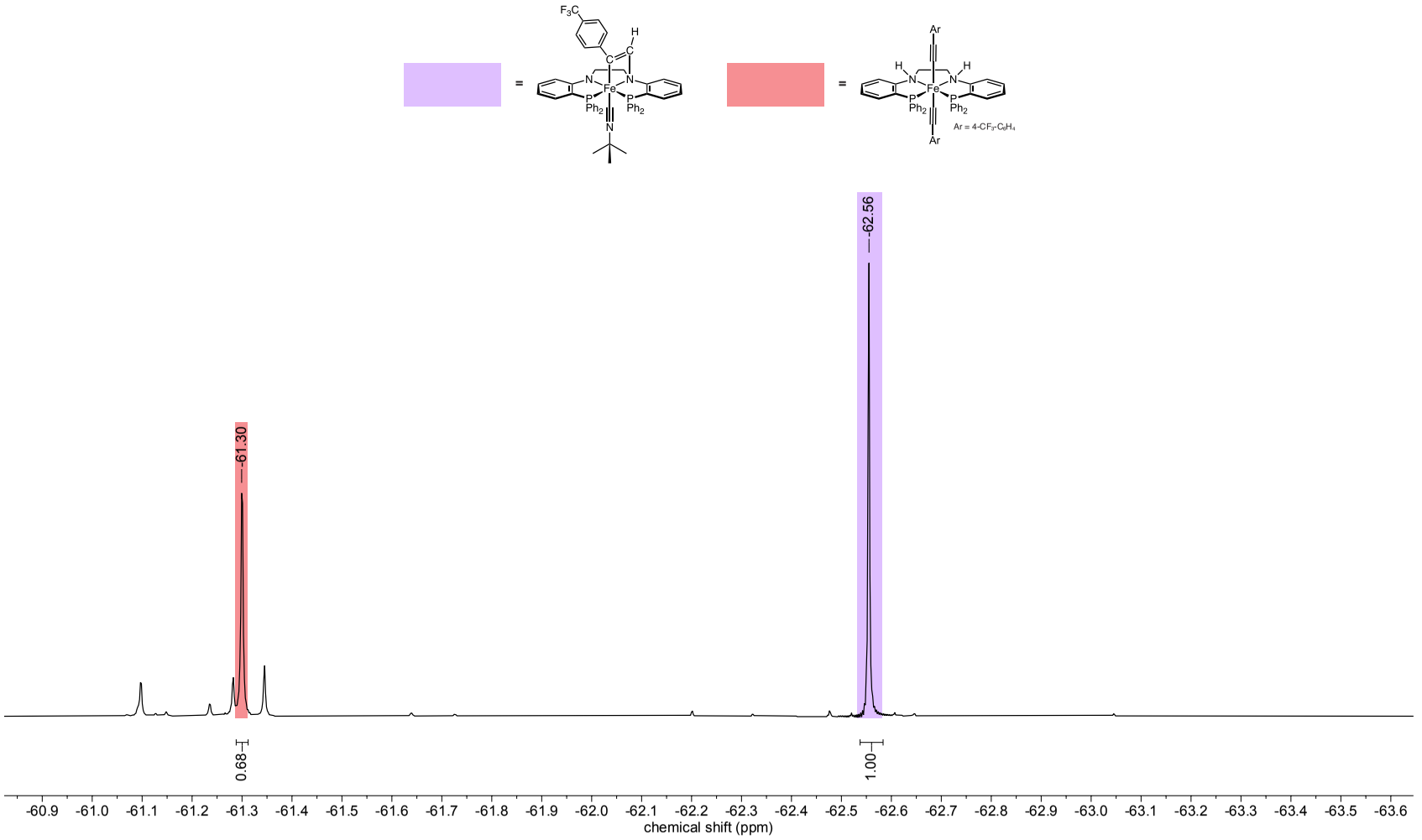

Figure S9: $^{19}F\{^{1}H\}$ NMR spectrum (C_6D_6, 376.5 MHz) resulting from the treatment of the **5** + **6** mixture with 1.0 equiv CN^tBu.

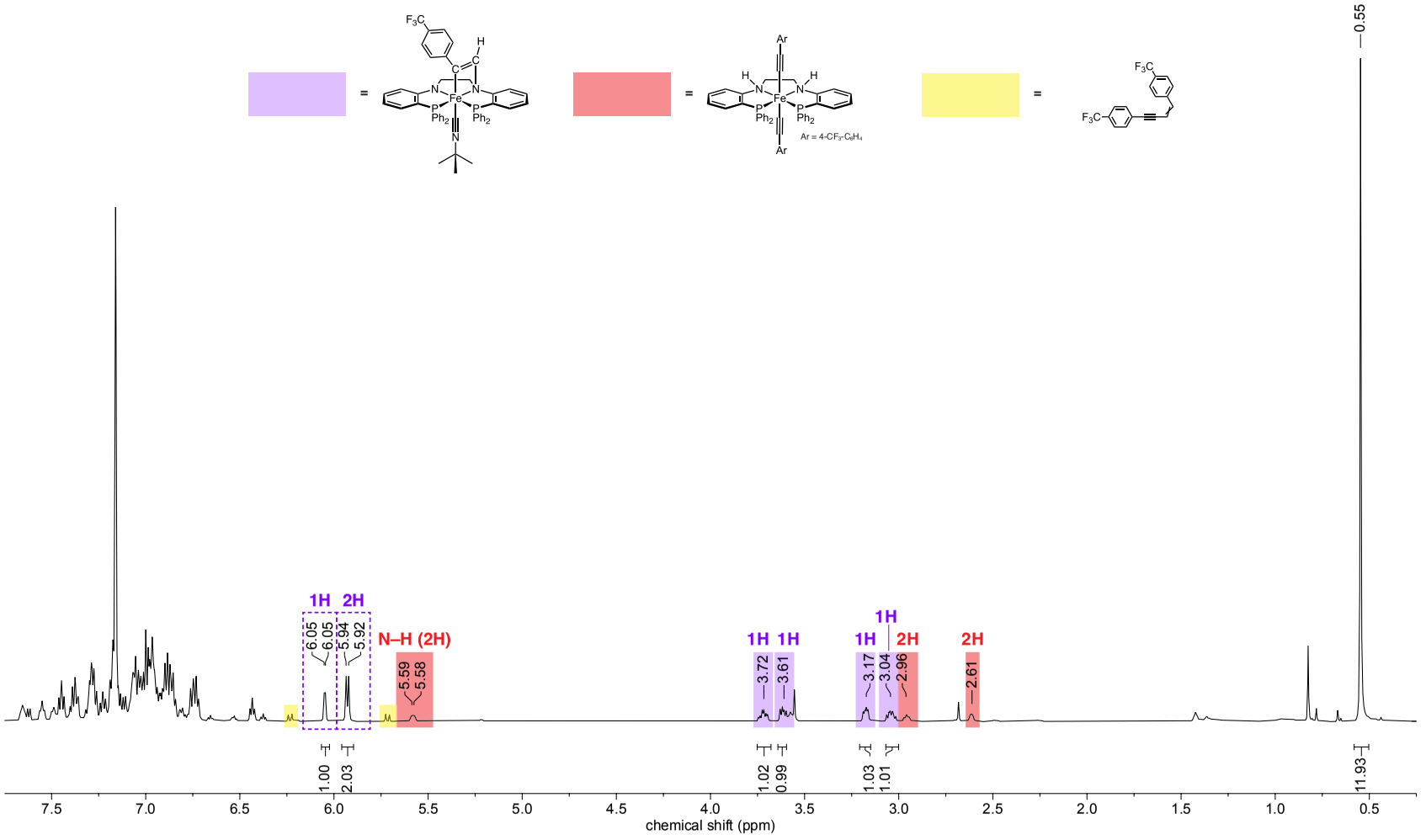

Figure S10: ^{1}H NMR spectrum (C_6D_6, 400 MHz) resulting from the treatment of the **5** + **6** mixture with 1.0 equiv CN^{t}Bu. The numbers given in violet/red text by each highlighted resonance refer to the number of H to which each resonance corresponds on **6** and **5**, respectively.

4 Additional Data

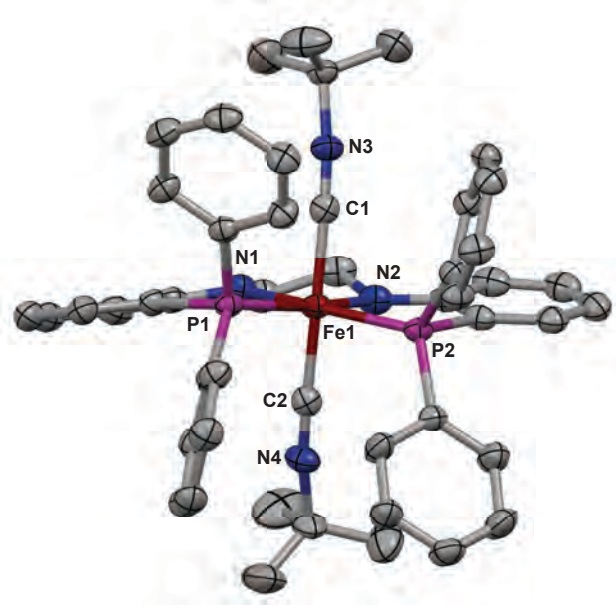

Figure S11: Displacement ellipsoid (50%) representation of **3**. For clarity, carbon-bonded H atoms and rotational disorder of the *tert*-butyl methyl groups are omitted. Relevant atomic distances (Å) and angles (°): Fe1–N1: 1.9941(15), Fe1–N2: 1.9907(15), Fe1–P1: 2.2293(5), Fe1–P2: 2.2244(5), Fe1–C1: 1.8691(18), Fe1–C2: 1.8530(18), C1–N3: 1.160(2), C2–N4: 1.162(2), C1–Fe1–C2: 171.90(7).

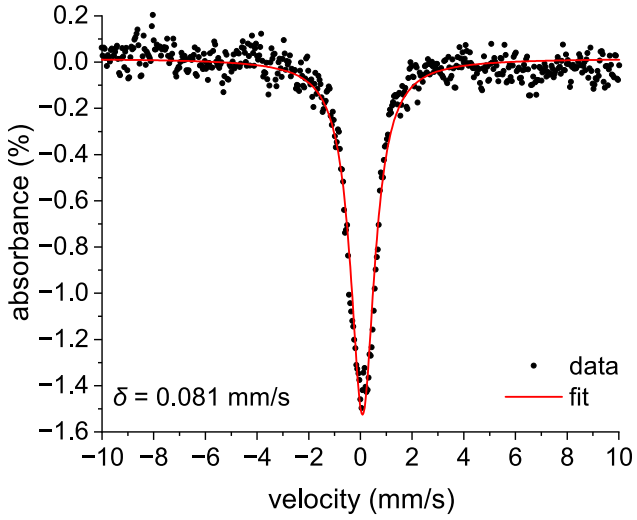

Figure S12: Fitted ^{57}Fe Mössbauer spectrum (4 K) of **3**.

Table S1: Summary of X-Ray diffraction experimental details and refined parameters for **2**, **3**, **6**, and **5**.

	2 · 4 (C_6H_5F)	**3**	(**5** + **6**) · Et_2O	**7**
Formula	$C_{78}H_{64}F_4FeN_2P_2$	$C_{48}H_{50}FeN_4P_2$	$C_{60}H_{52}F_6FeN_2P_2O$	$C_{52}H_{46}F_3FeN_3P_2$
FW (g/mol)	1223.10	800.71	1048.82	887.71
T (K)	100(2)	100(2)	100(2)	100(2)
λ (Å)	0.71073	0.71073	0.71073	0.71073
a (Å)	29.4666(15)	10.7765(8)	13.4659(8)	11.7110(5)
b (Å)	13.8824(7)	13.6127(9)	13.8415(8)	12.5996(5)
c (Å)	16.5411(7)	14.6156(10)	14.7796(9)	16.8271(8)
α (°)	90	90.015(2)	93.4090(19)	96.3440(14)
β (°)	114.2120(14)	96.865(3)	105.088 (2)	100.6083(15)
γ (°)	90	100.703(2)	106.3324(18)	116.0944(13)
V (Å^3)	6171.2(5)	2091.1(3)	2526.2(3)	2139.53(16)
Space Group	$C2/c$	$P\bar{1}$	$P\bar{1}$	$P\bar{1}$
Z	4	2	2	2
D_{calcd} (g/cm^3)	1.316	1.272	1.379	1.378
μ (mm^{-1})	0.356	0.475	0.429	0.481
R_1 ($I > 2\sigma(I)$)	0.0311	0.324	0.0455	0.0323
wR_2 (all data)	0.0855	0.0890	0.1240	0.0855

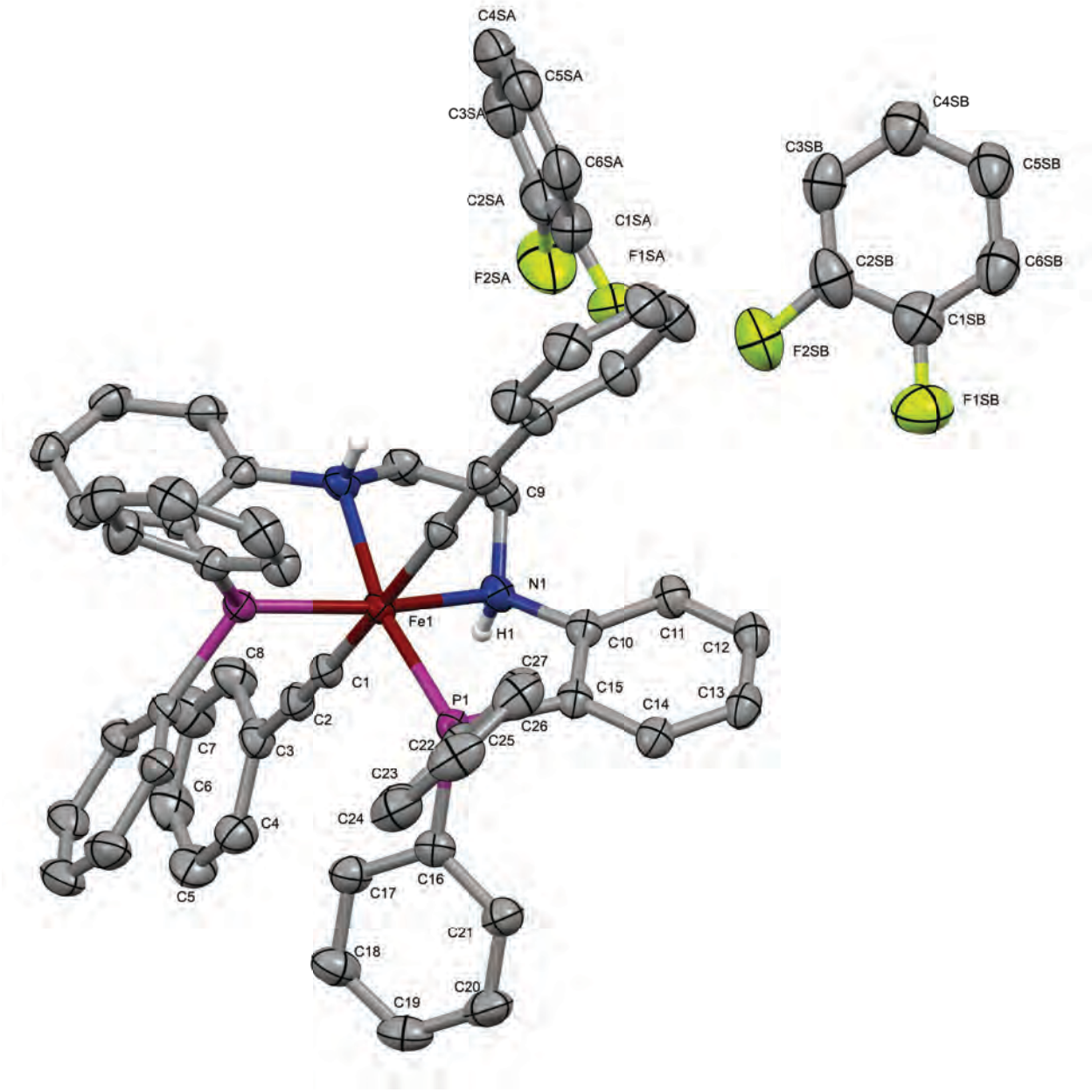

Figure S13: Fully-labeled displacement ellipsoid (50%) representation of **2**. Symmetry-equivalent positions of the asymmetric unit are generated to provide a complete molecular representation. The fluorobenzene solvent molecules are each disordered over two positions.

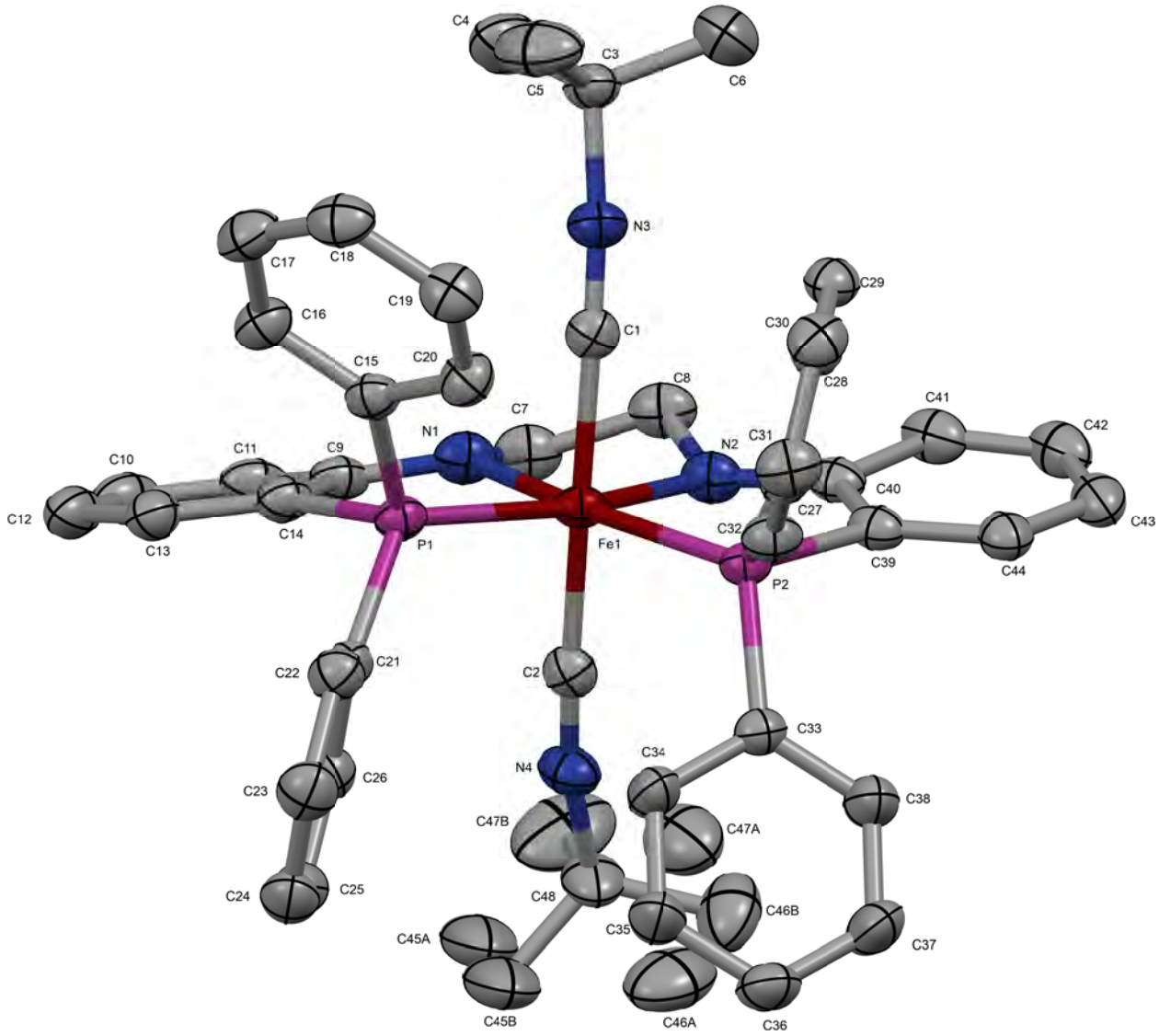

Figure S14: Fully-labeled displacement ellipsoid (50%) representation of **3**.

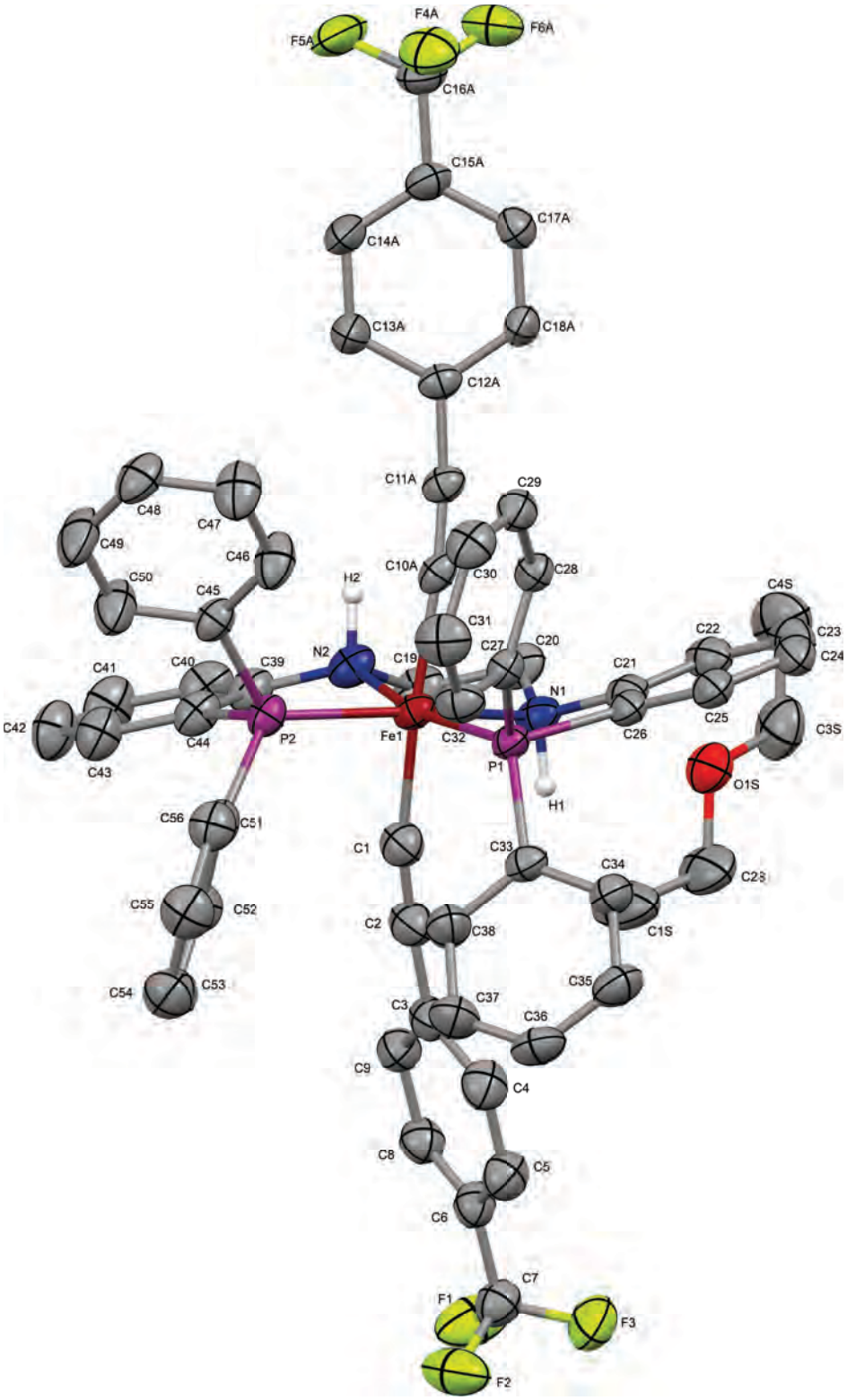

Figure S15: Fully-labeled displacement ellipsoid (50%) representation of **5** obtained as the major component (75%) co-crystallized with **6** (Figure S16).

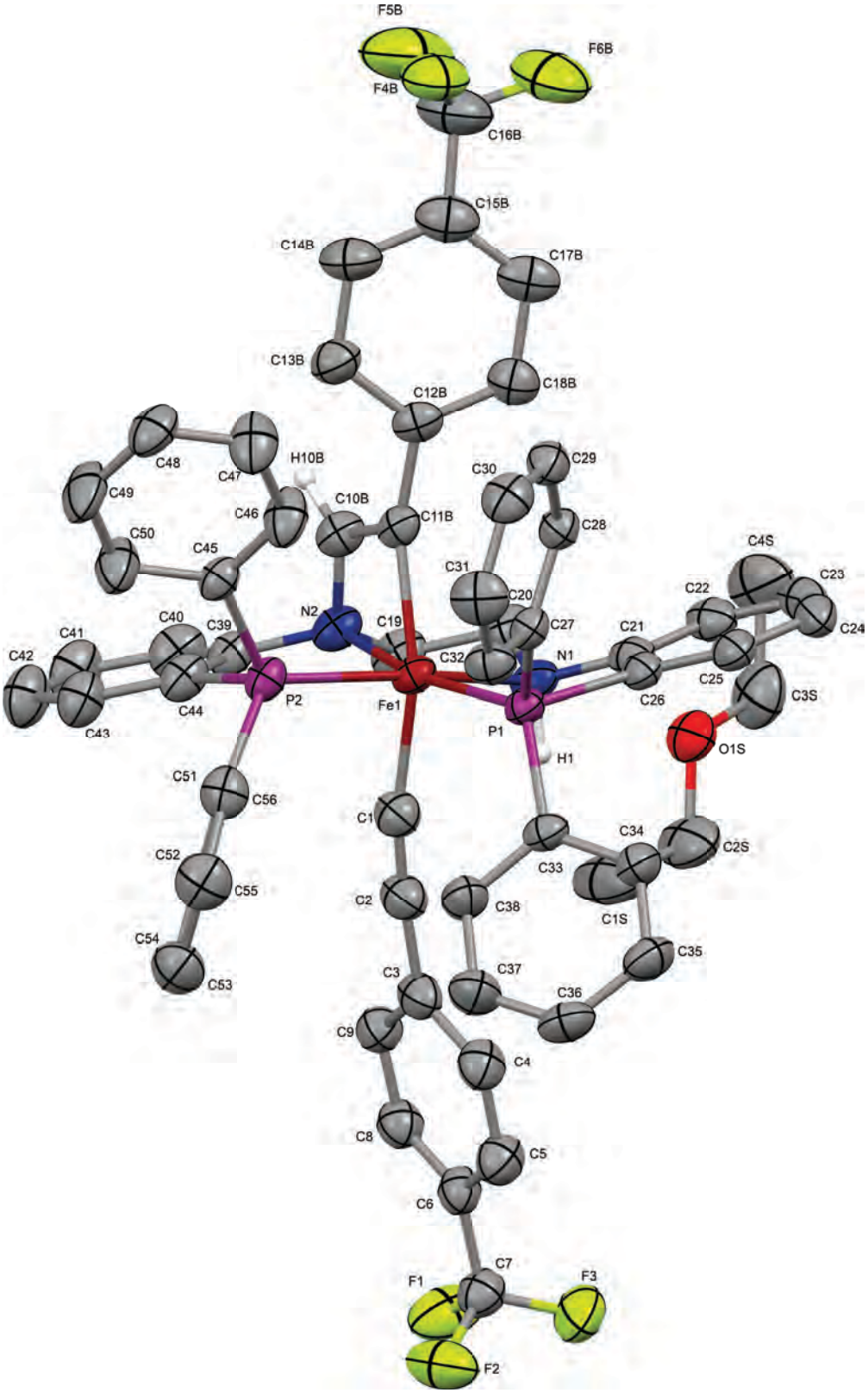

Figure S16: Fully-labeled displacement ellipsoid (50%) representation of **6** obtained as the minor component (25%) co-crystallized with **5** (**??**).

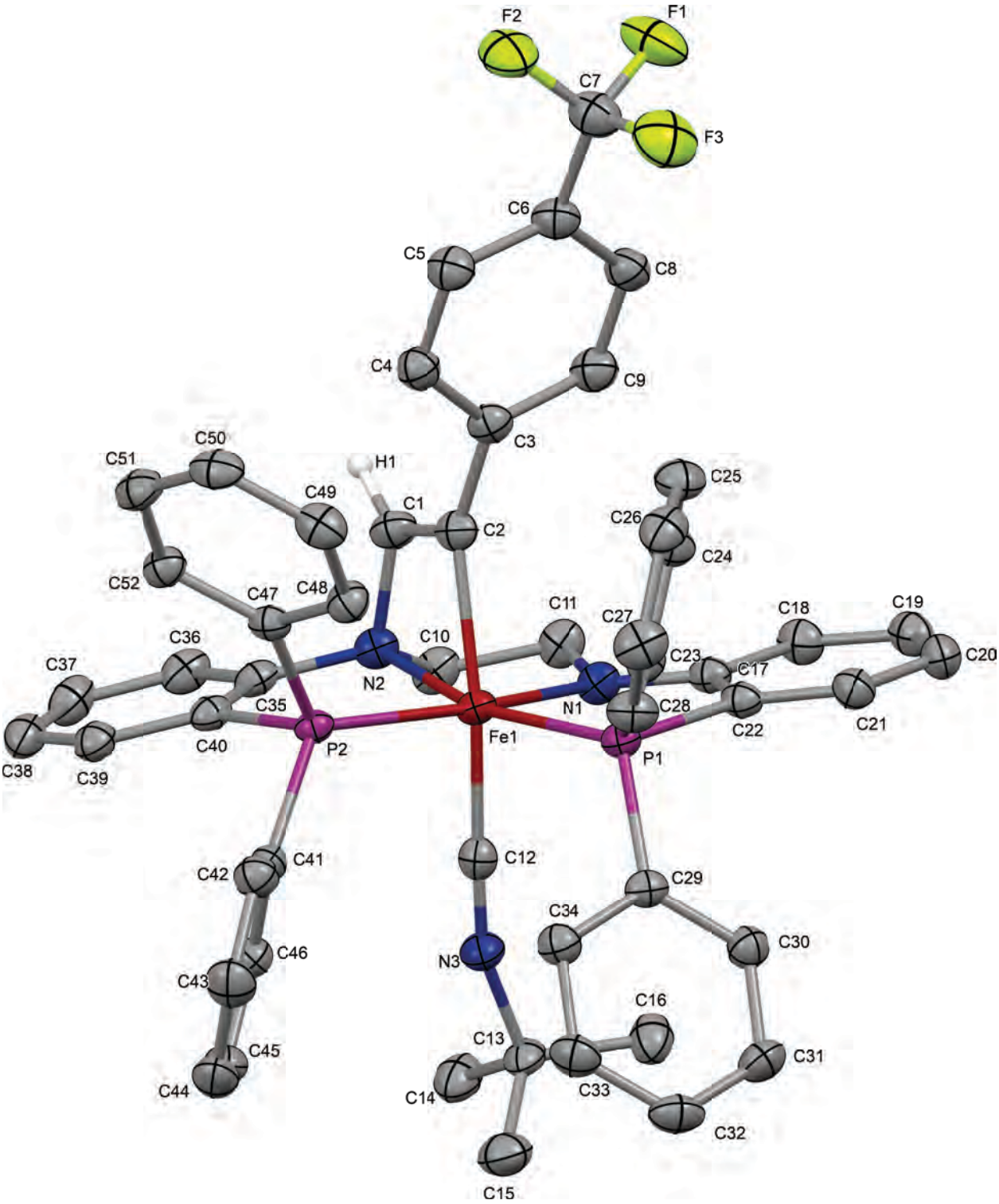

Figure S17: Fully-labeled displacement ellipsoid (50%) representation of **7**.

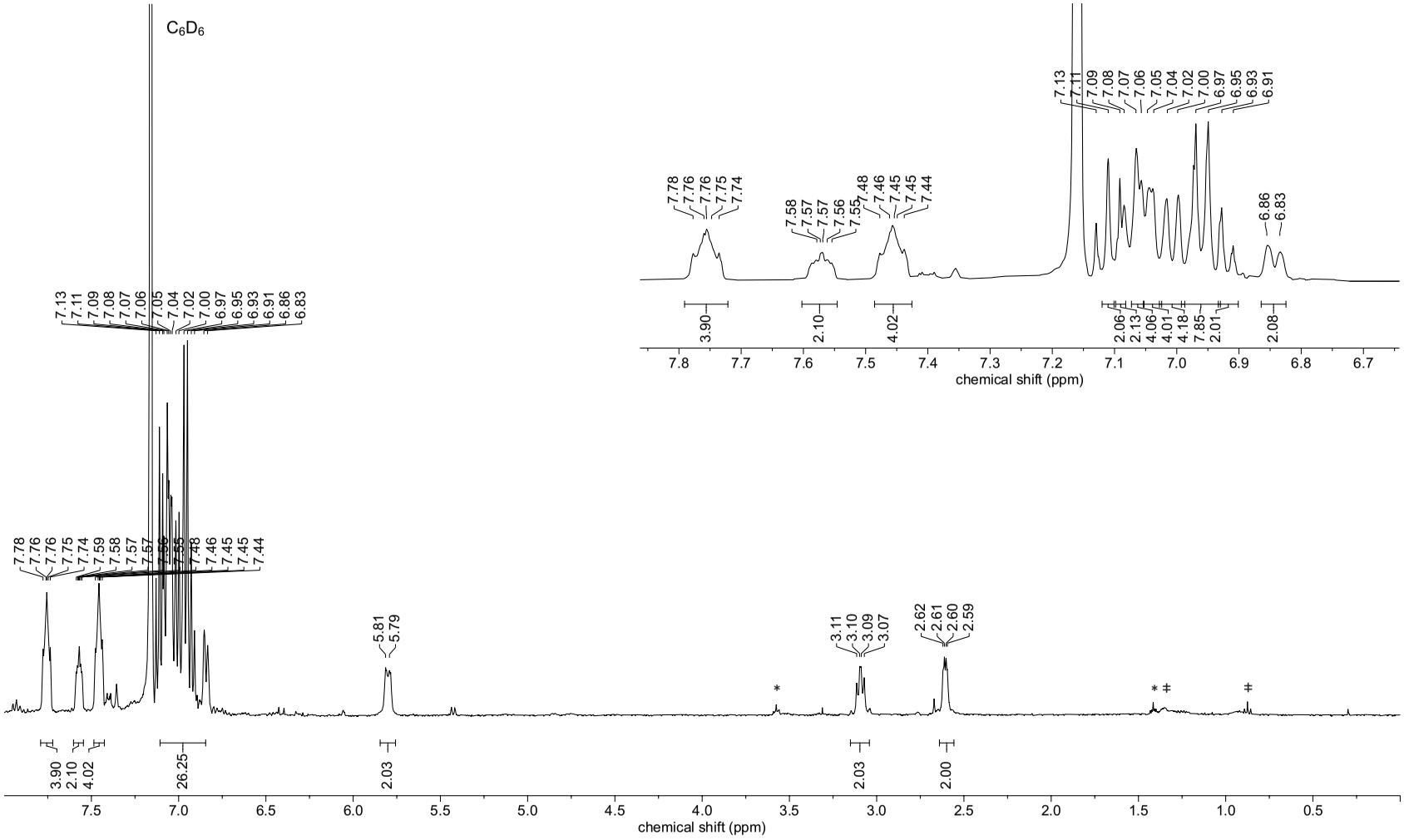

Figure S18: ^{1}H NMR spectrum (C_6D_6, 400 MHz) of **2**. Residual THF and pentane are marked with ∗ and ‡, respectively.

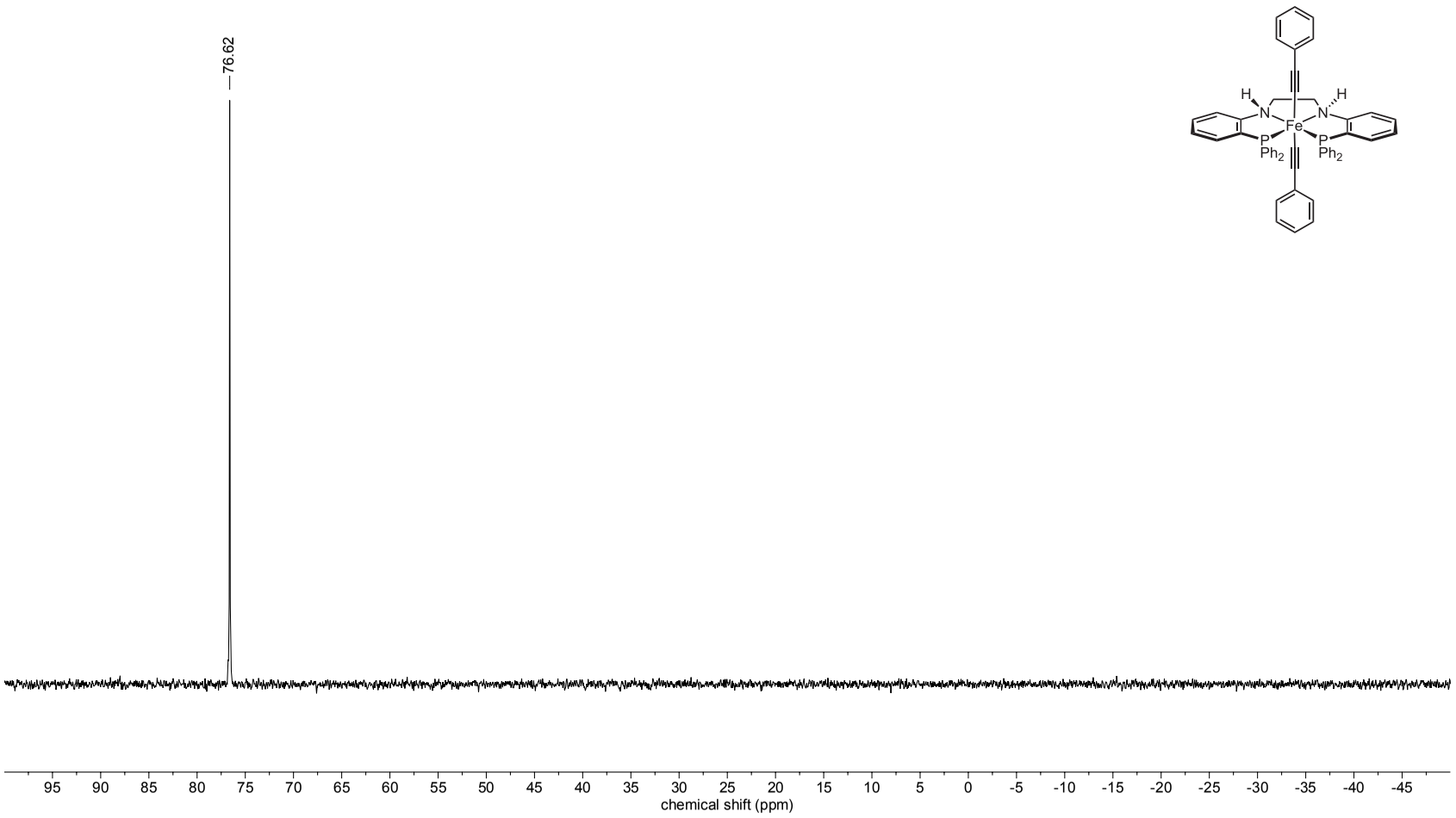

Figure S19: $^{31}P\{^{1}H\}$ NMR spectrum (C_6D_6, 243 MHz) of **2**.

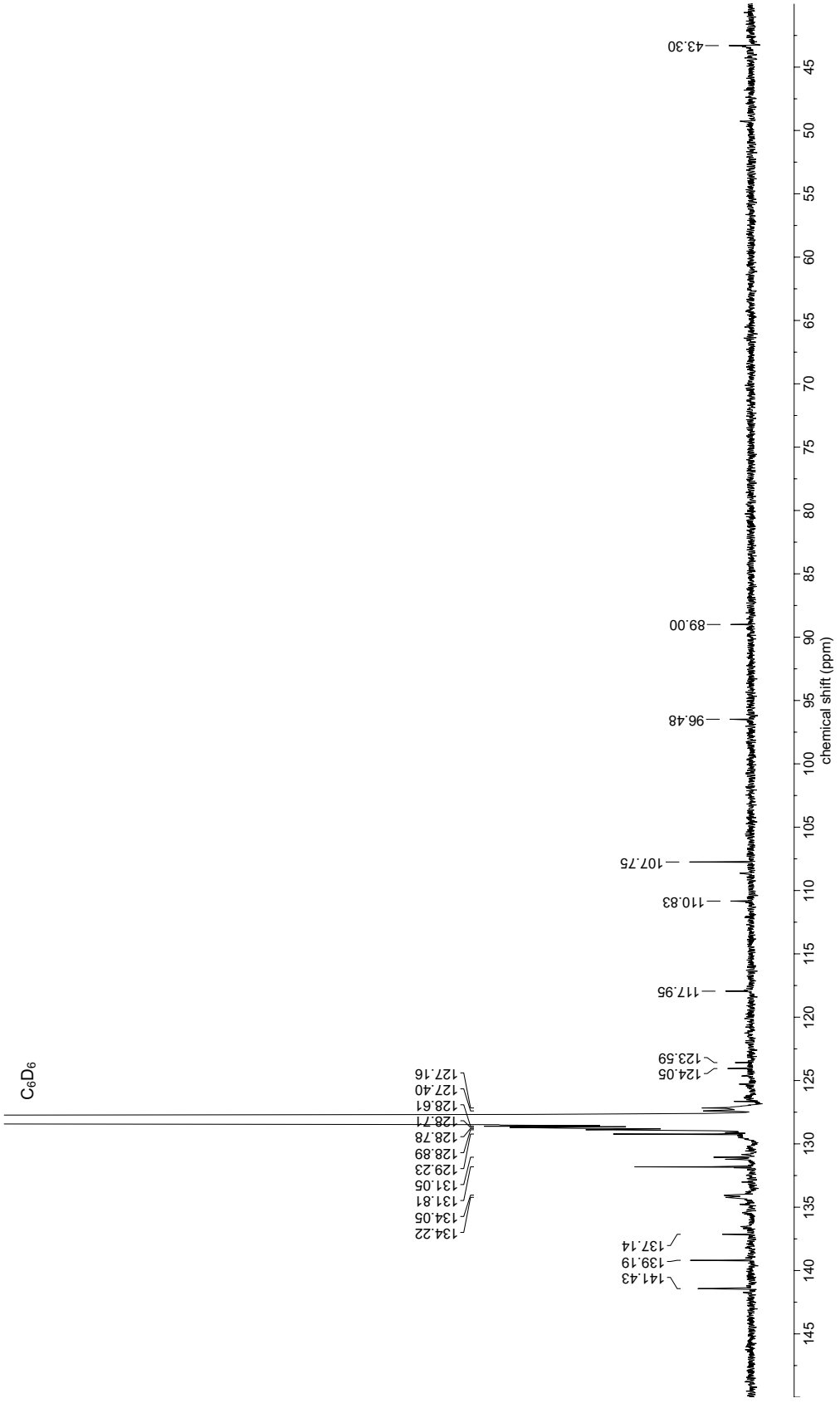

Figure S20: $^{13}C\{^{1}H\}$ NMR spectrum (C_6D_6, 101 MHz) of **2**.

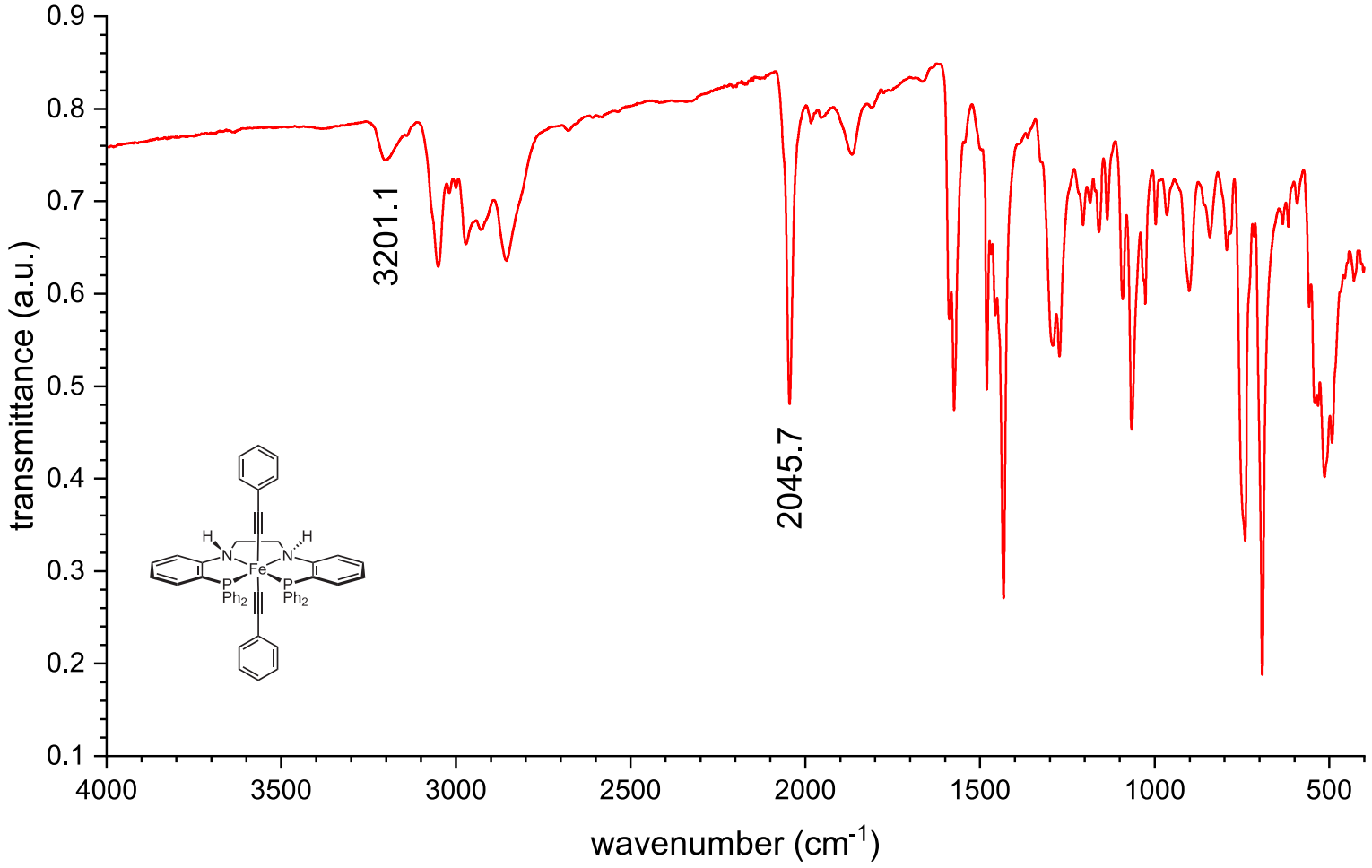

Figure S21: ATR-IR spectrum of **2**.

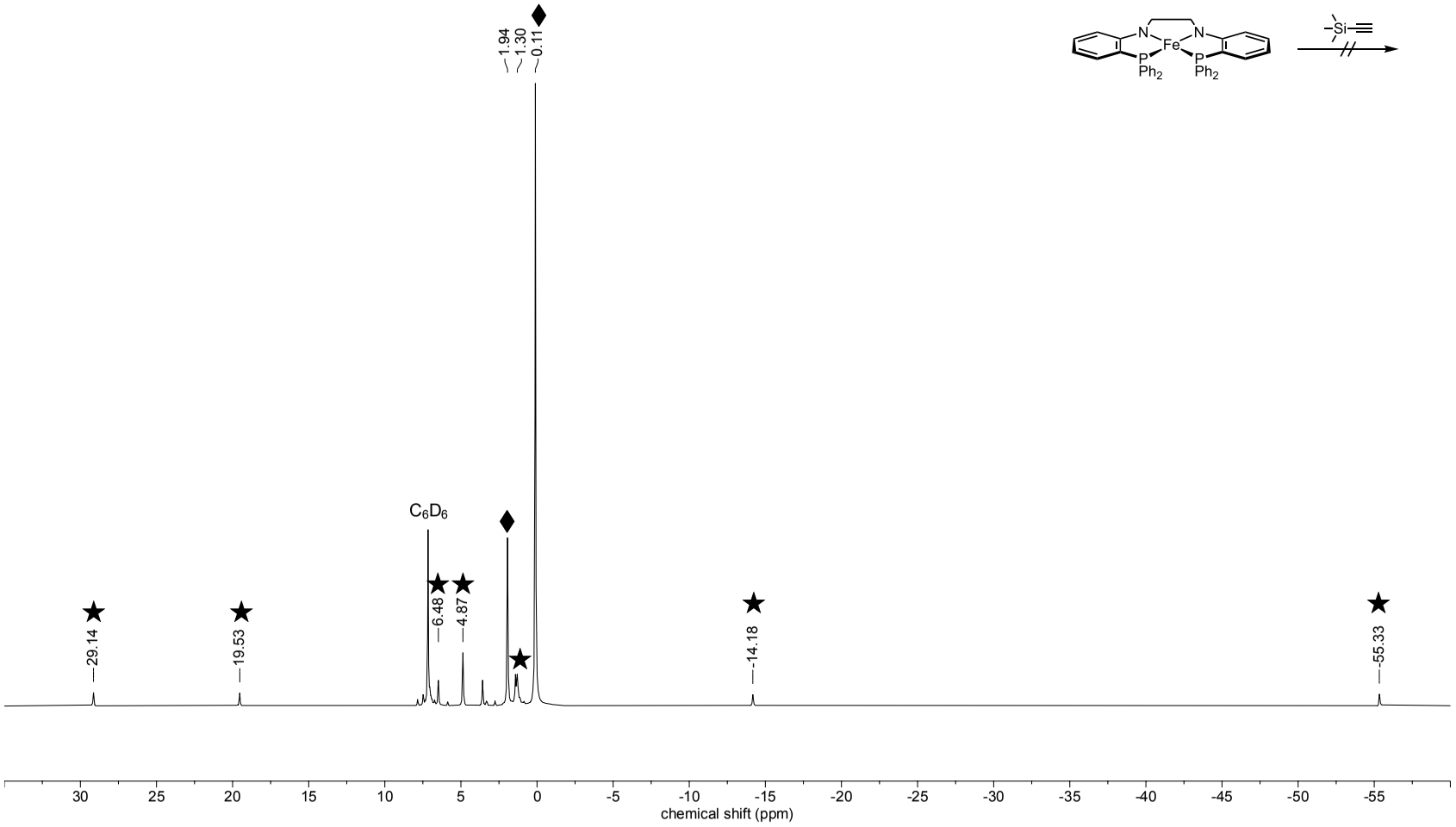

Figure S22: ^{1}H NMR spectrum (C_6D_6, 400 MHz) of the attempted reaction of **1** (★) with TMSCCH (⧫).

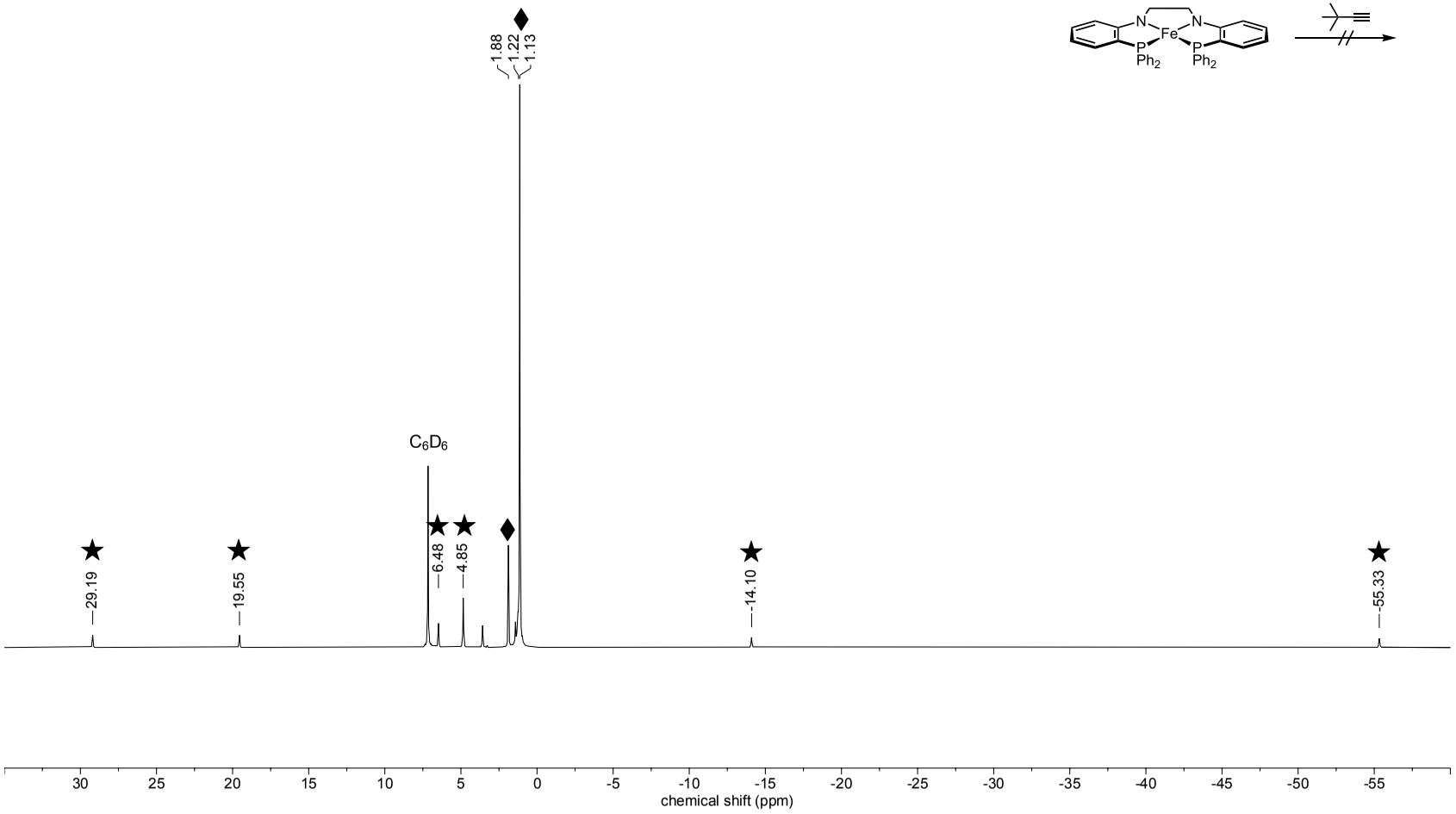

Figure S23: ^{1}H NMR spectrum (C_6D_6, 400 MHz) of the attempted reaction of **1** (★) with ^{t}BuCCH (⧫).

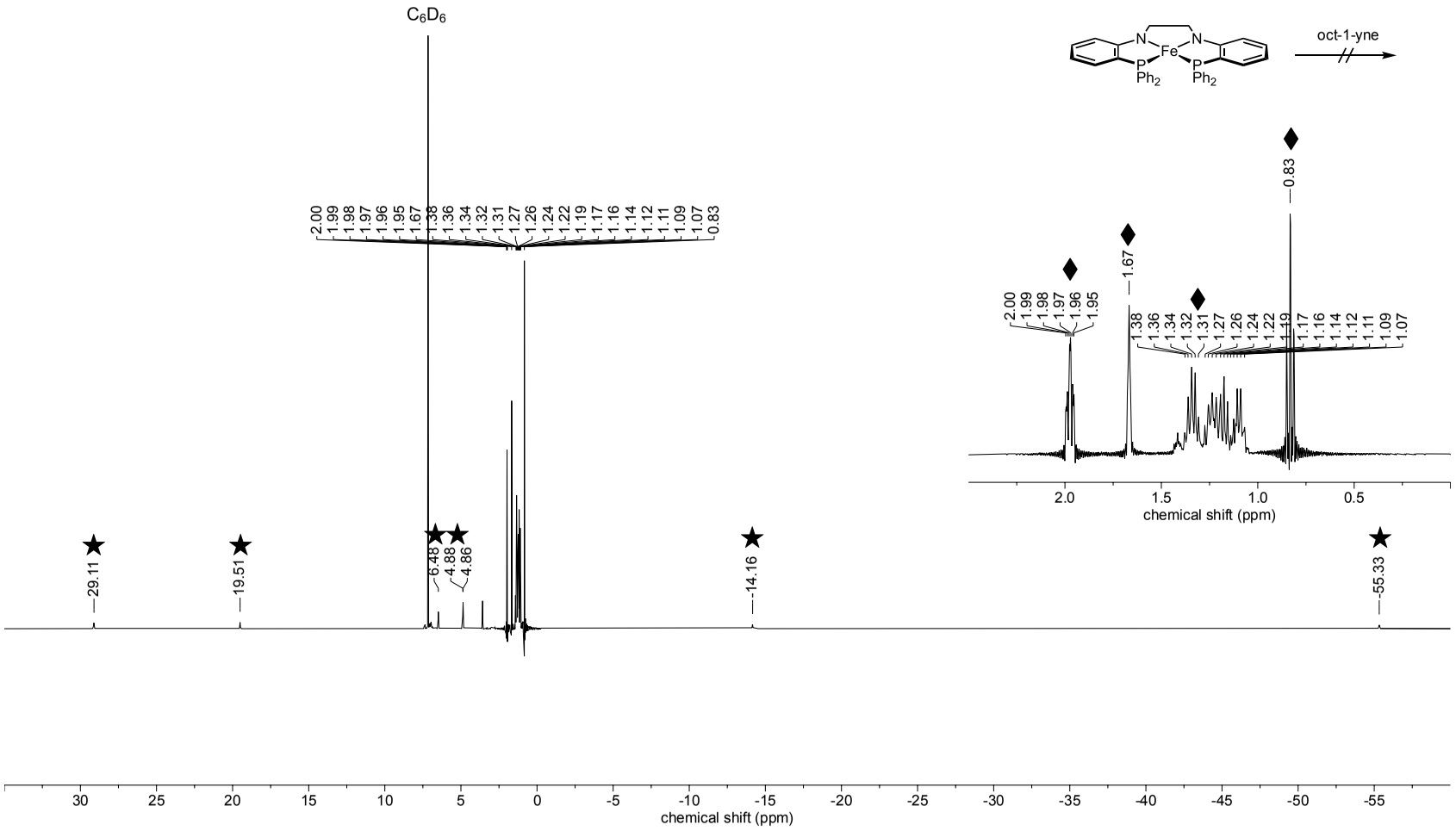

Figure S24: ^{1}H NMR spectrum (C_6D_6, 400 MHz) of the attempted reaction of **1** (★) with 1-octyne (♦).

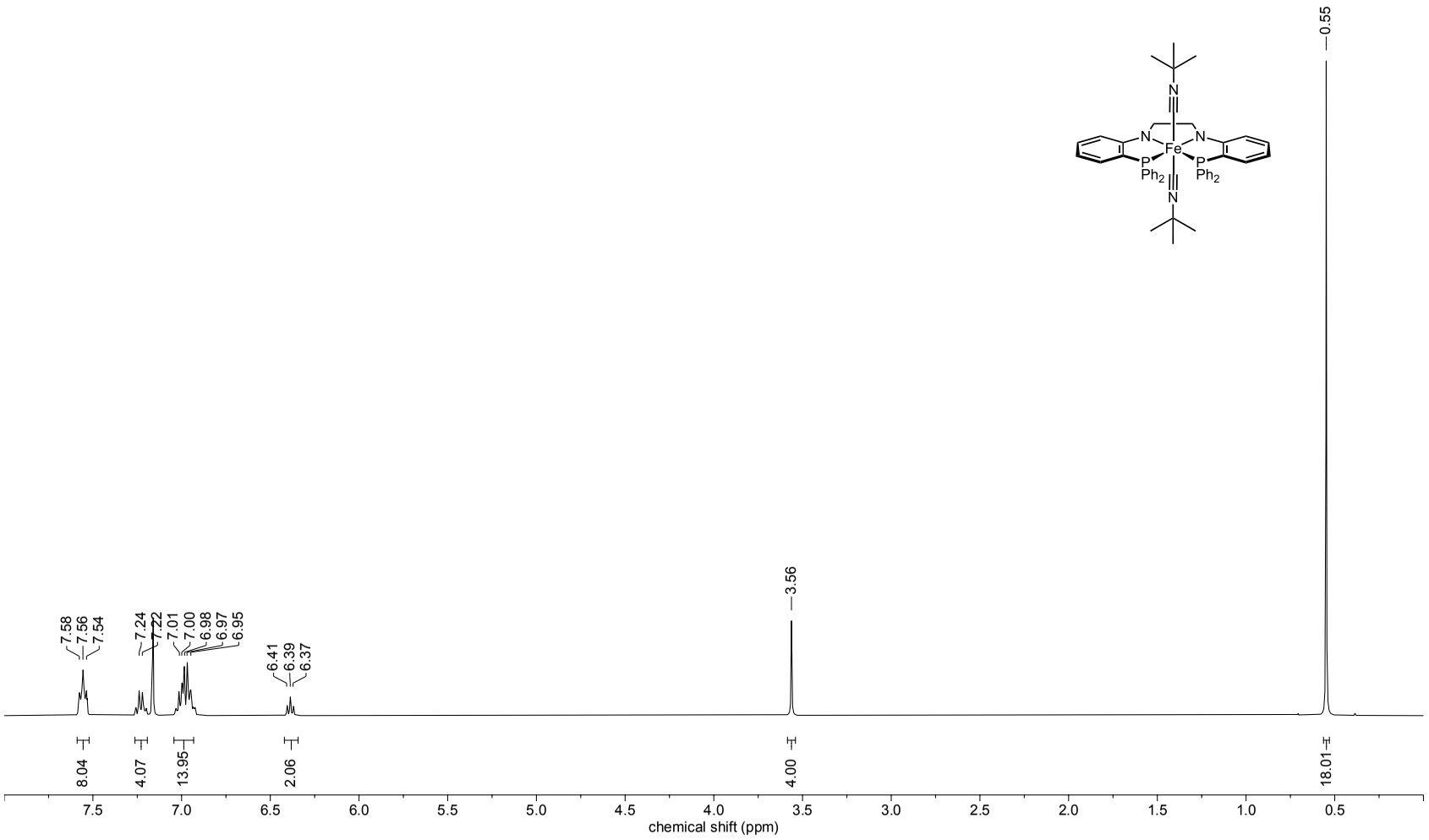

Figure S25: ^{1}H NMR spectrum (C_6D_6, 400 MHz) of **3**.

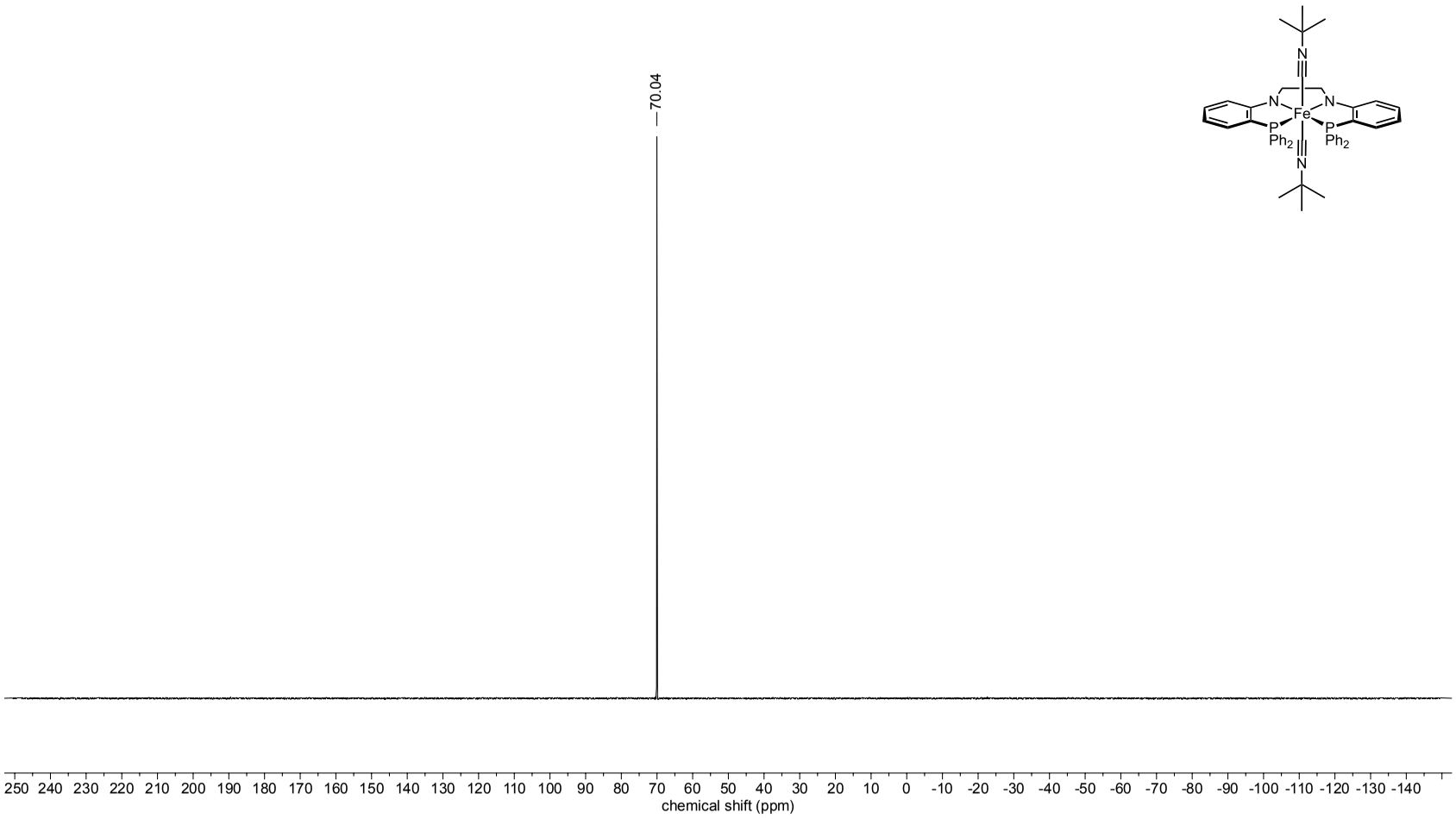

Figure S26: $^{31}P\{^{1}H\}$ NMR spectrum (C_6D_6, 243 MHz) of **3**.

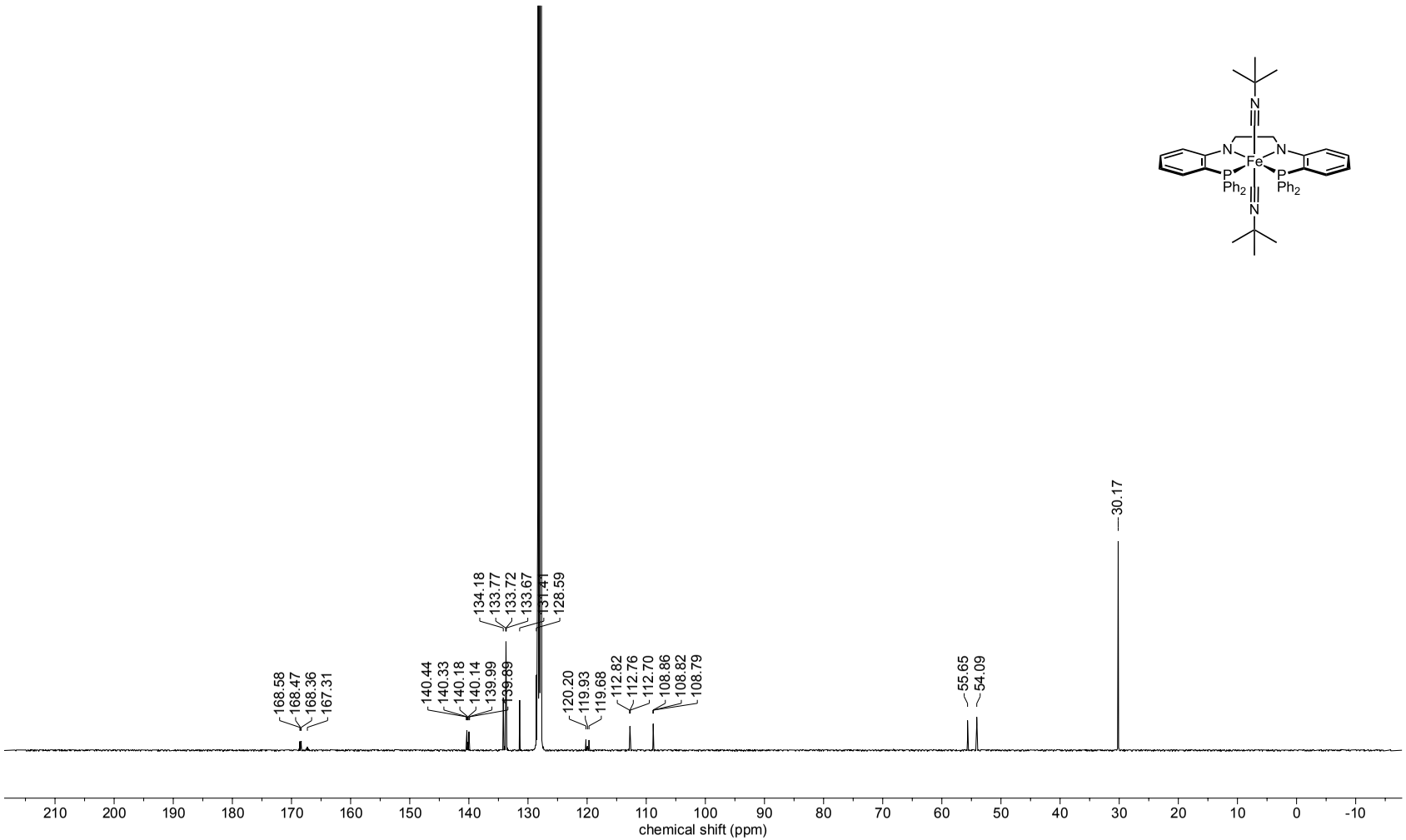

Figure S27: $^{13}C\{^{1}H\}$ NMR spectrum (C_6D_6, 101 MHz) of **3**.

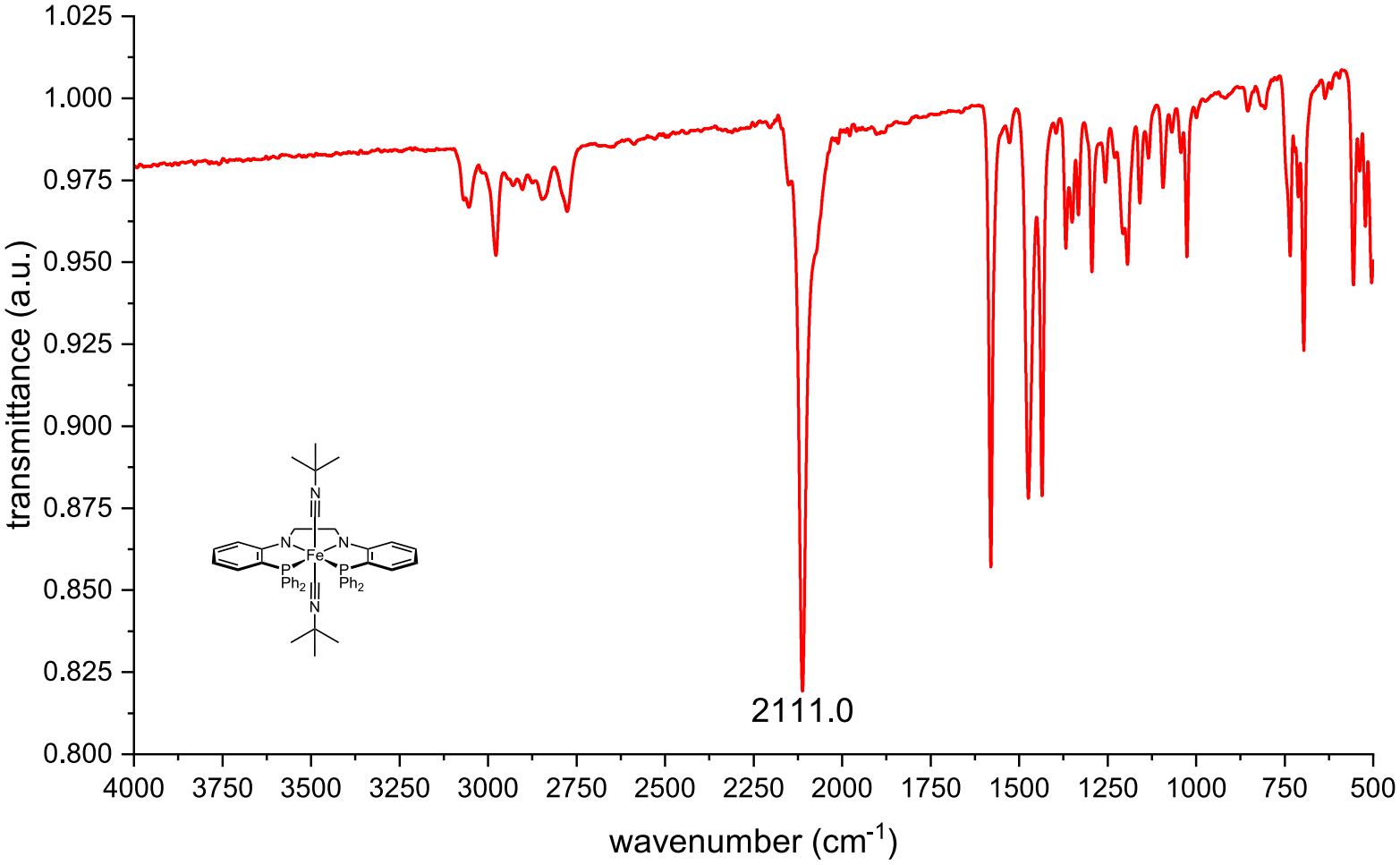

Figure S28: ATR-IR spectrum of **3**.

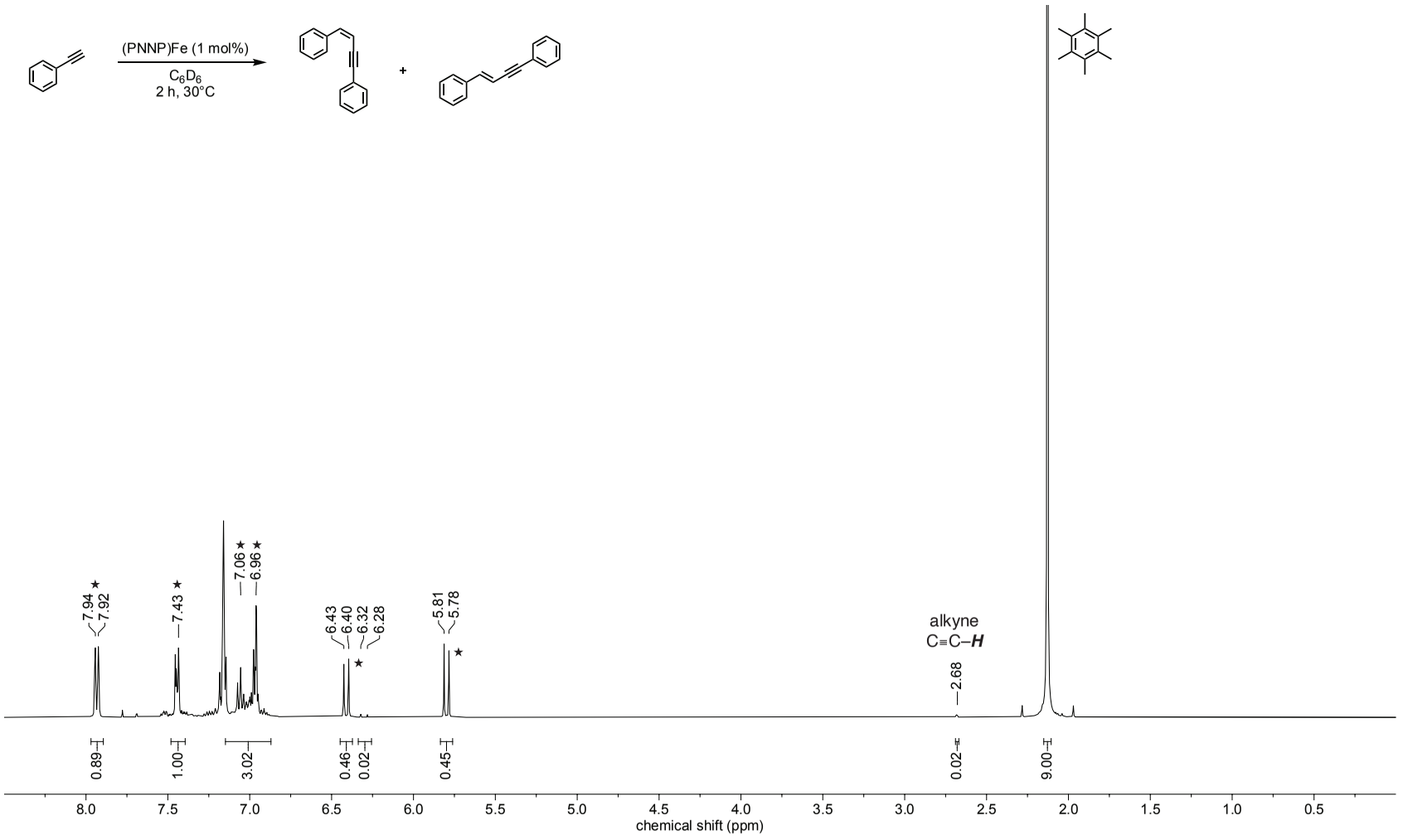

Figure S29: Quantitative ^{1}H NMR spectrum (C_6D_6, 400 MHz) of the reaction of **1** with 95 equiv PhCCH. Peaks corresponding to the organic dimer are labeled with ∗.

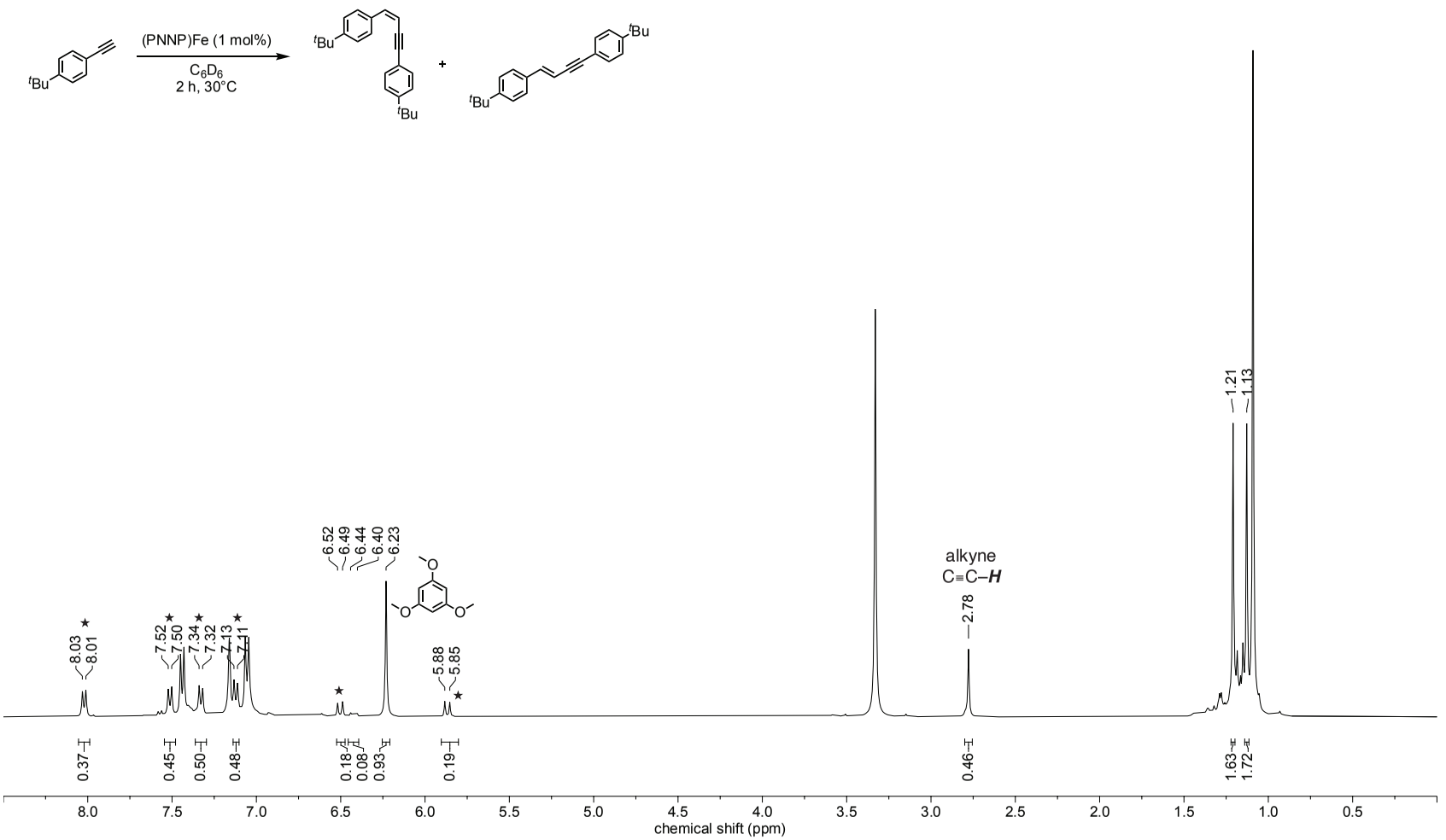

Figure S30: Quantitative ^{1}H NMR spectrum (C_6D_6, 400 MHz) of the reaction of **1** with 95 equiv 4-^{t}Bu-PhCCH. Peaks corresponding to the organic dimer are labeled with $*$.

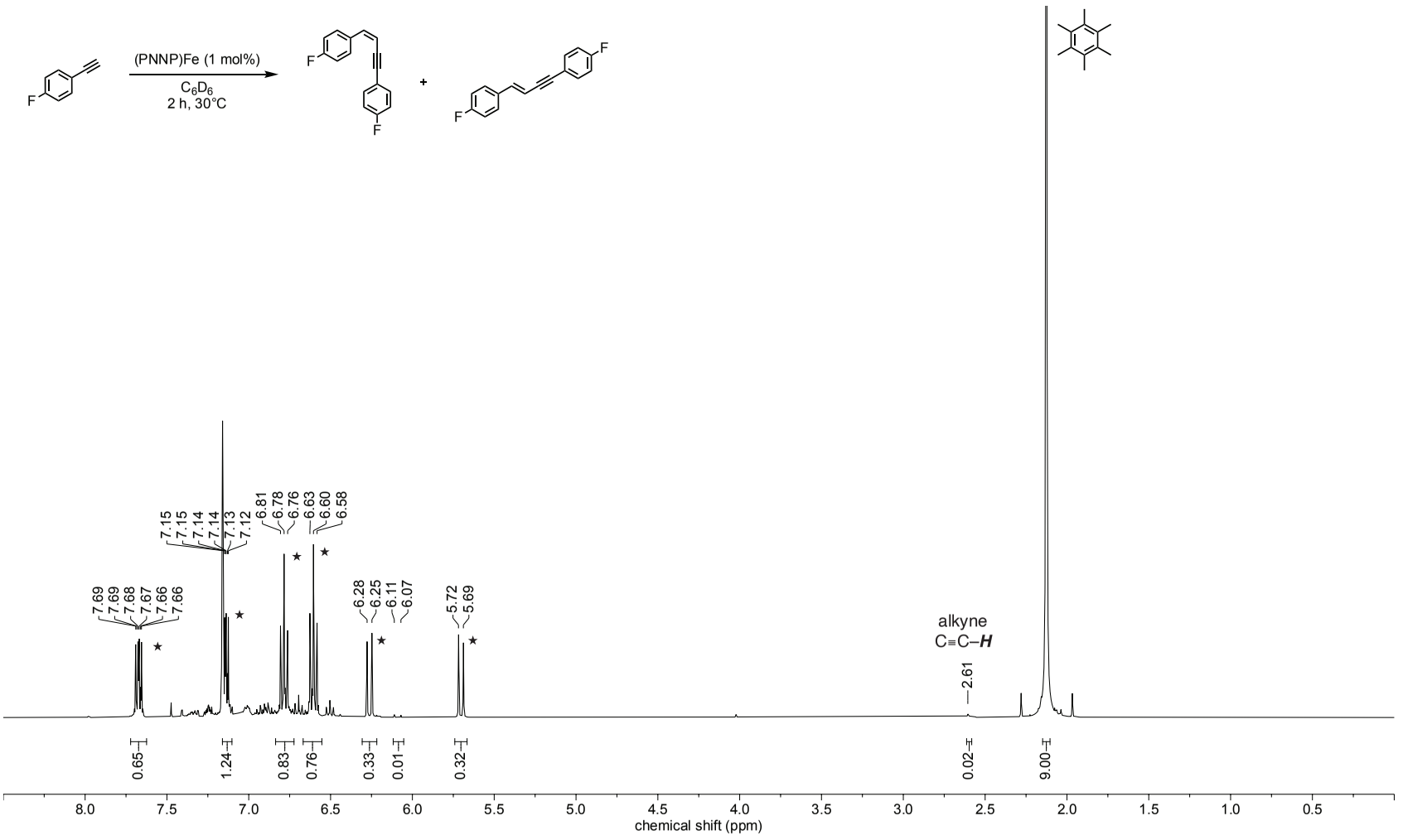

Figure S31: Quantitative ^{1}H NMR spectrum (C_6D_6, 400 MHz) of the reaction of **1** with 95 equiv 4-F-PhCCH. Peaks corresponding to the organic dimer are labeled with ∗.

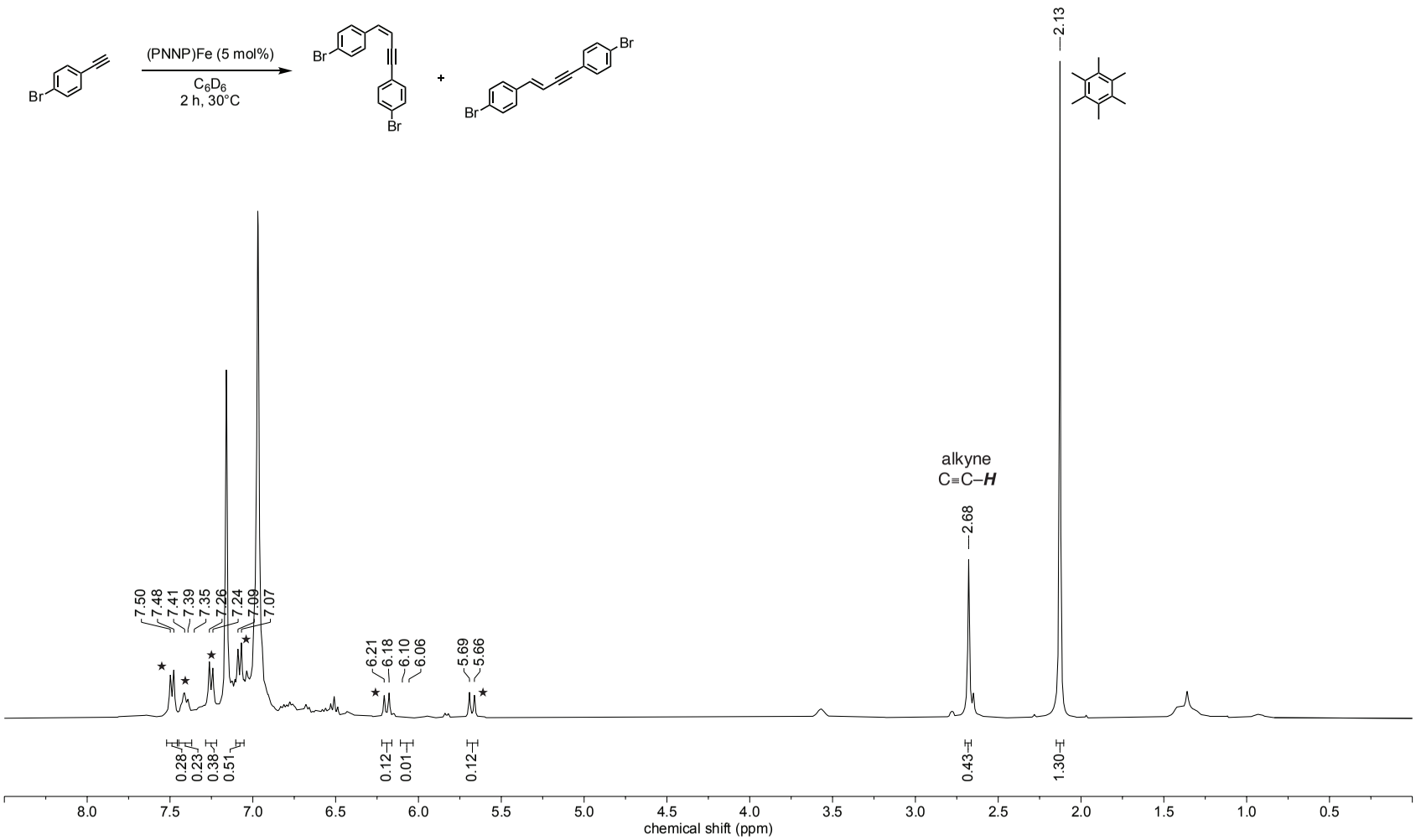

Figure S32: Quantitative ^{1}H NMR spectrum (C_6D_6, 400 MHz) of the reaction of **1** with 20 equiv 4-Br-PhCCH. Peaks corresponding to the organic dimer are labeled with ∗.

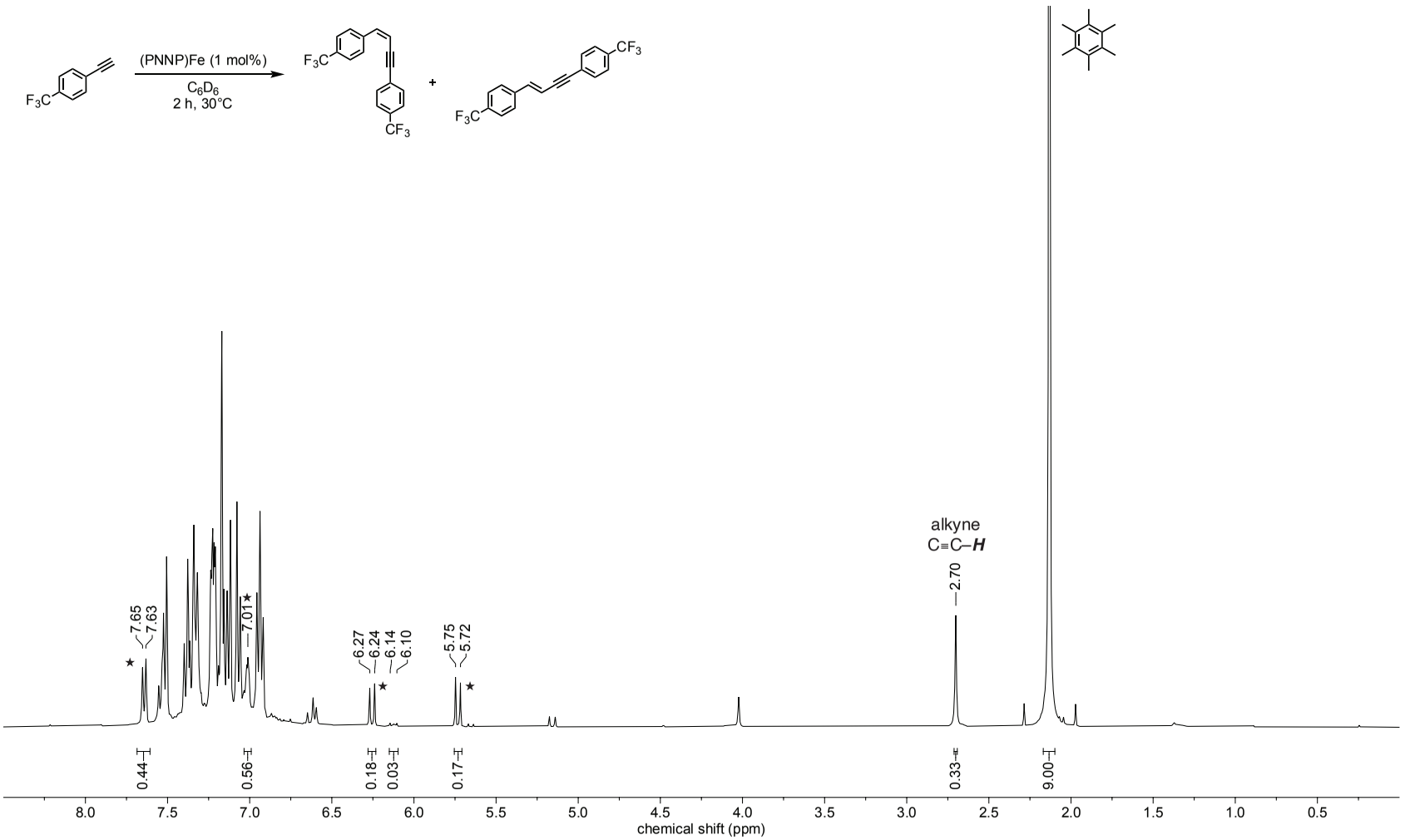

Figure S33: Quantitative ^{1}H NMR spectrum (C_6D_6, 400 MHz) of the reaction of **1** with 95 equiv 4-CF_3-PhCCH. Peaks corresponding to the organic dimer are labeled with $*$.

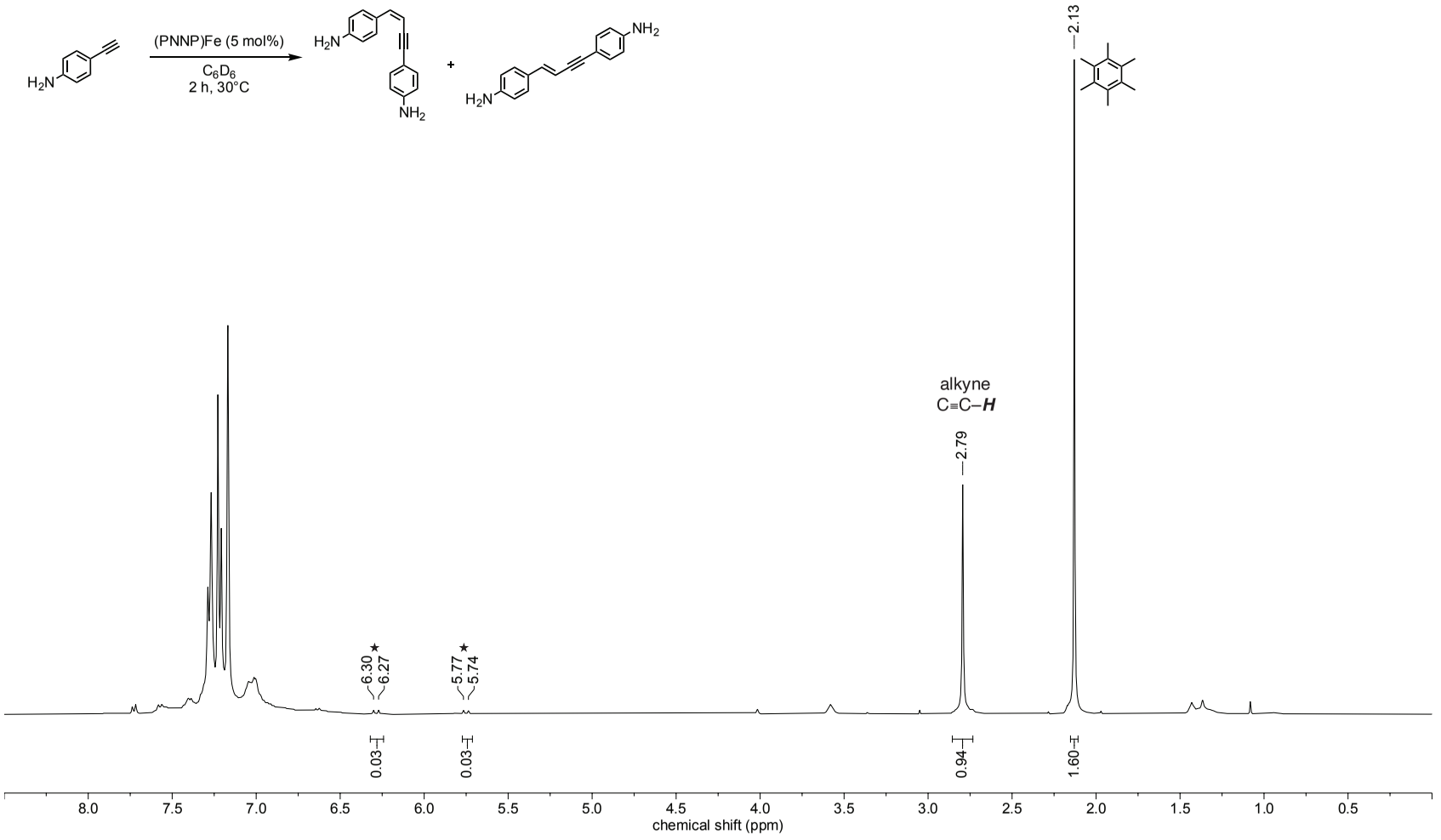

Figure S34: Quantitative ^{1}H NMR spectrum (C_6D_6, 400 MHz) of the reaction of **1** with 20 equiv 4-NH_2-PhCCH. Peaks corresponding to the organic dimer are labeled with $*$.

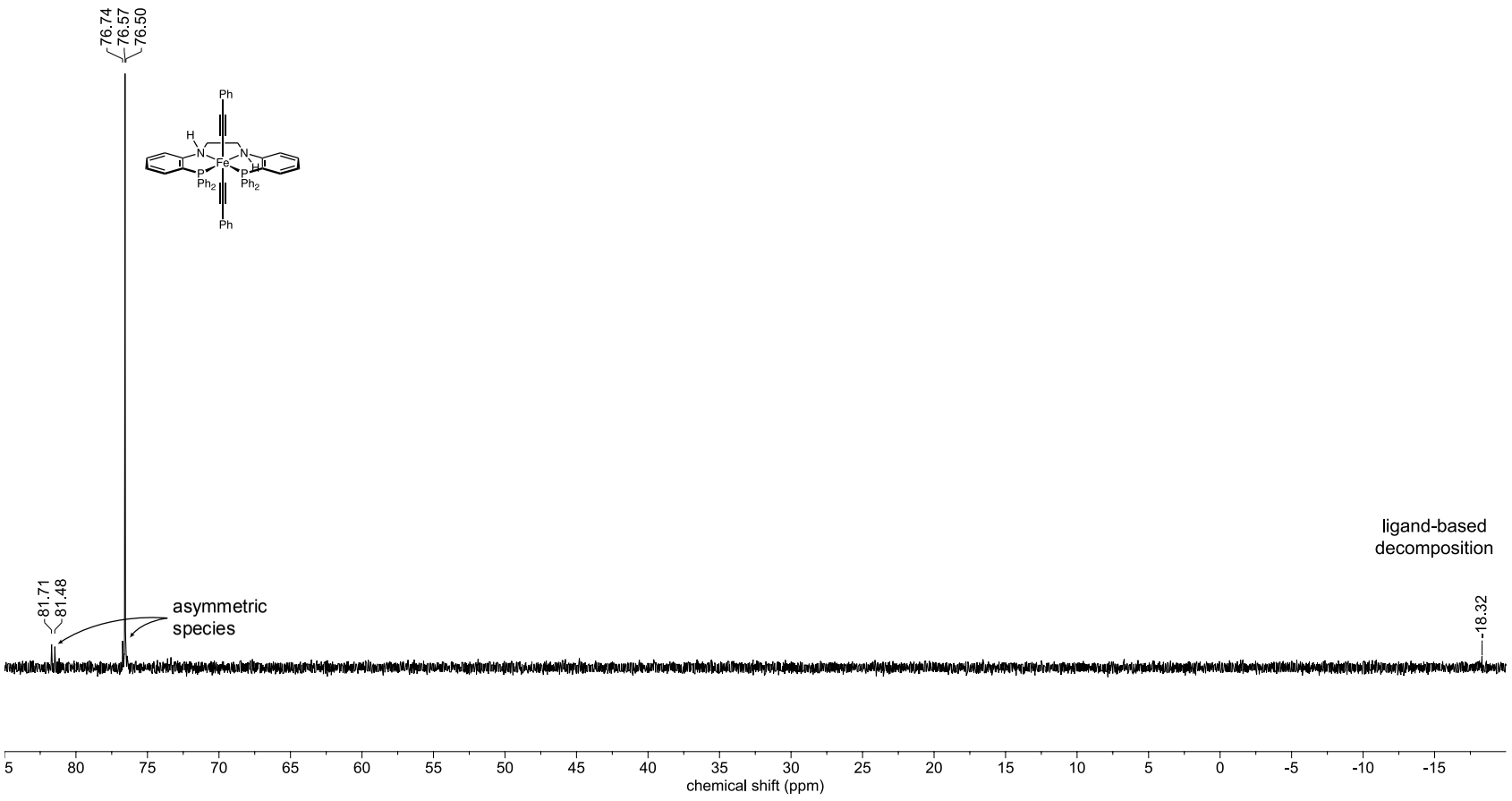

Figure S35: $^{31}P\{^{1}H\}$ NMR spectrum (THF, 243 MHz) of the crude catalytic mixture of **2** with 95 equiv PhCCH. Peaks present correspond to **2** (main peak), an asymmetric Fe-containing species (doublet of doublets; the rightmost doublet overlaps with the singlet), and ligand decomposition.

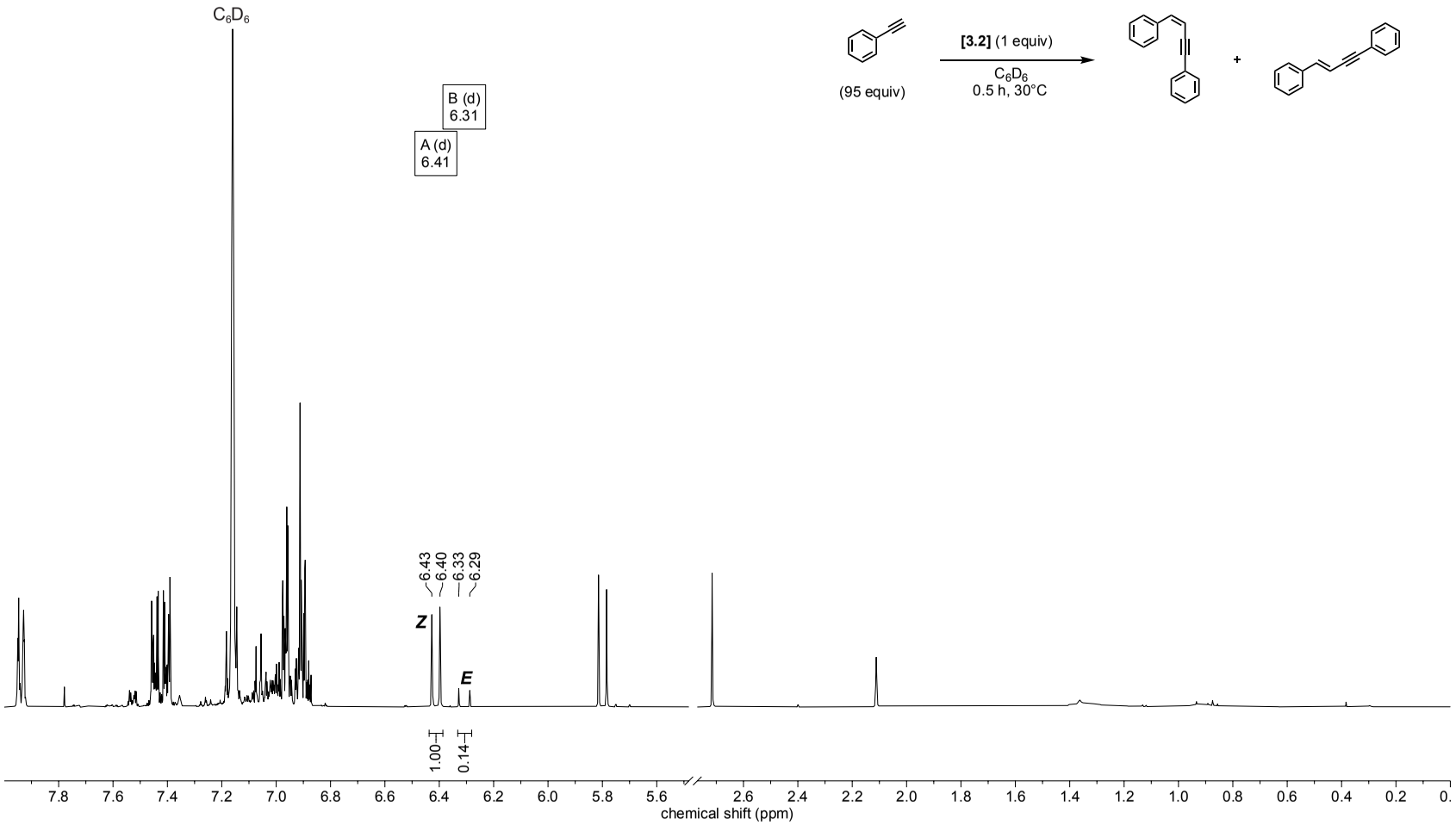

Figure S36: Quantitative ^{1}H NMR spectrum (C_6D_6, 400 MHz) of isolated organic products from the control reaction of **2** with 95 equiv PhCCH. Incomplete conversion is noted here due to shortened reaction time for the control reaction.

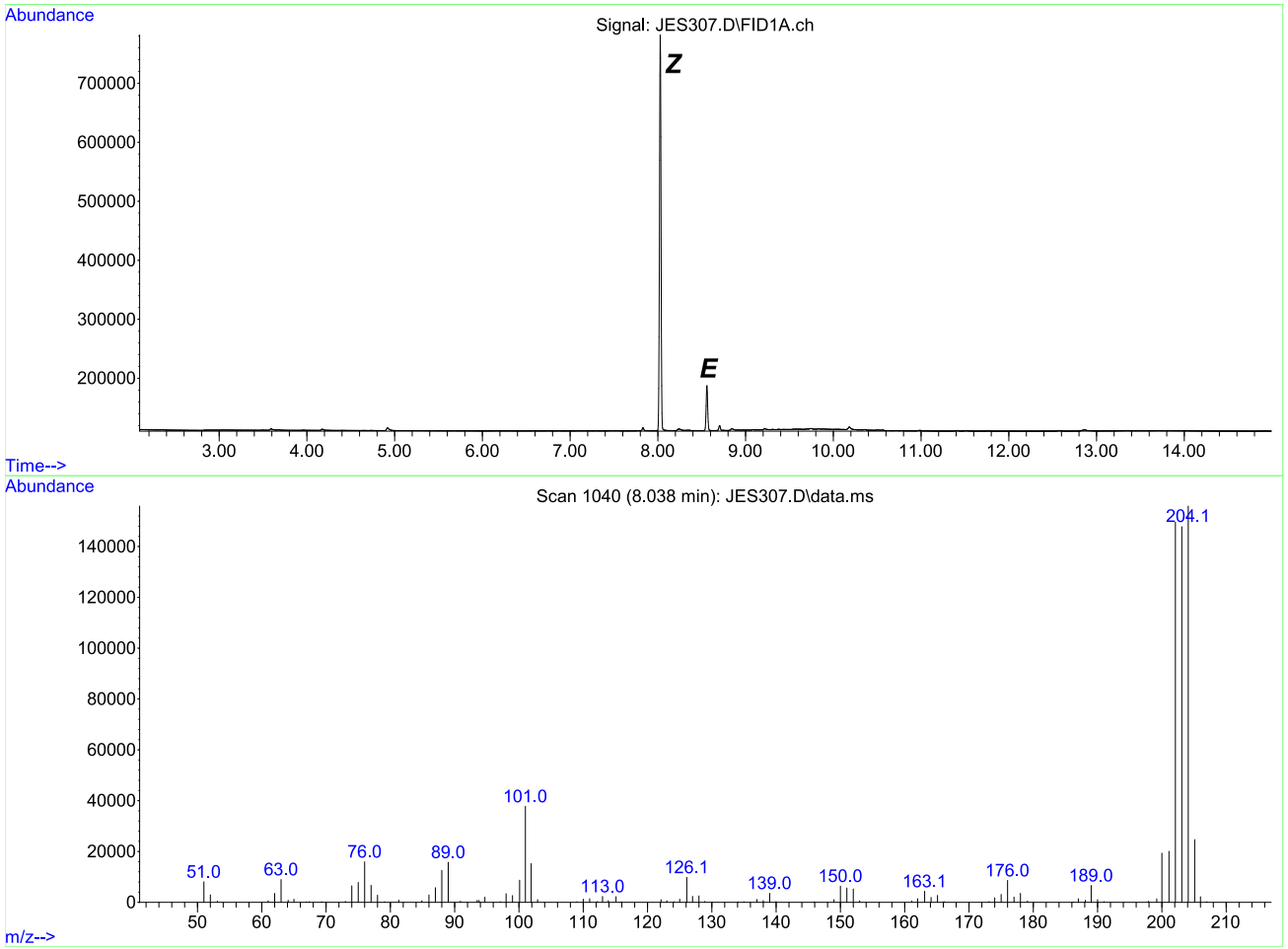

Figure S37: GC-FID chromatogram (top) and mass spectrum (bottom) of isolated organic products from the control reaction of **2** with 95 equiv PhCCH.

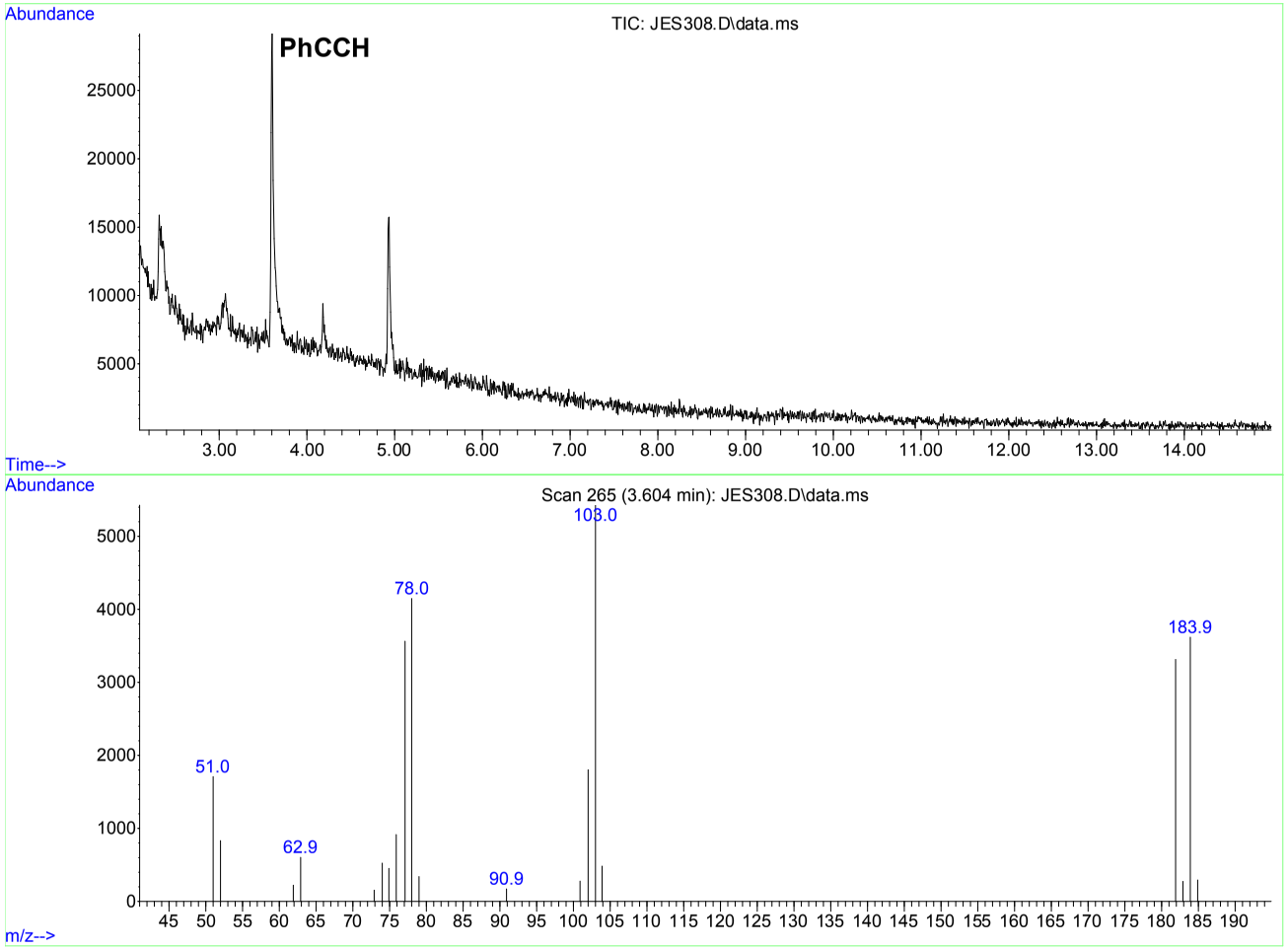

Figure S38: GC-MS chromatogram (top) and mass spectrum (bottom) of isolated organic products from the control reaction of $FeCl_2$ with 95 equiv PhCCH.

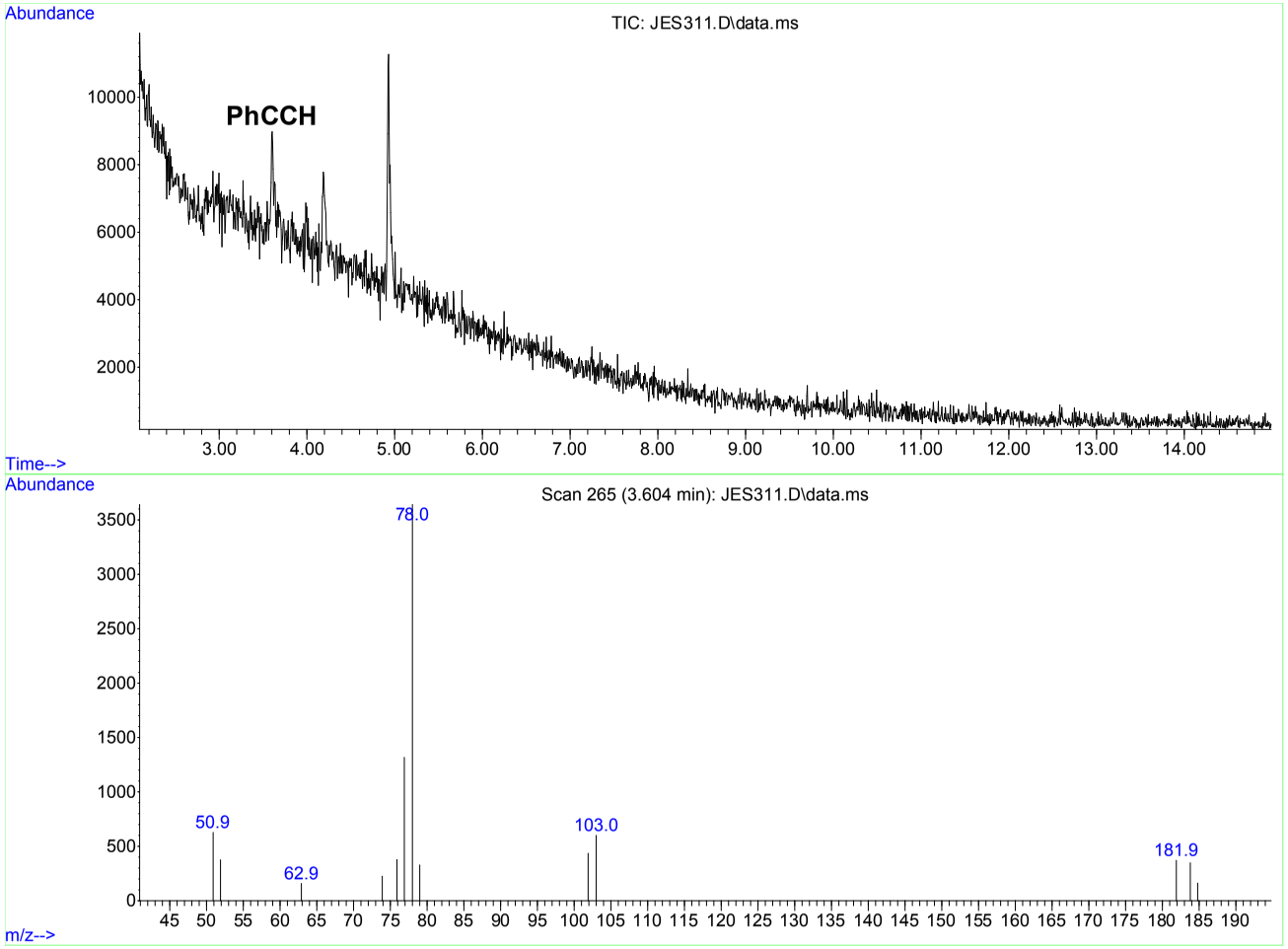

Figure S39: GC-MS chromatogram (top) and mass spectrum (bottom) of isolated organic products from the control reaction of $PN^{H}N^{H}P$ with 95 equiv PhCCH.

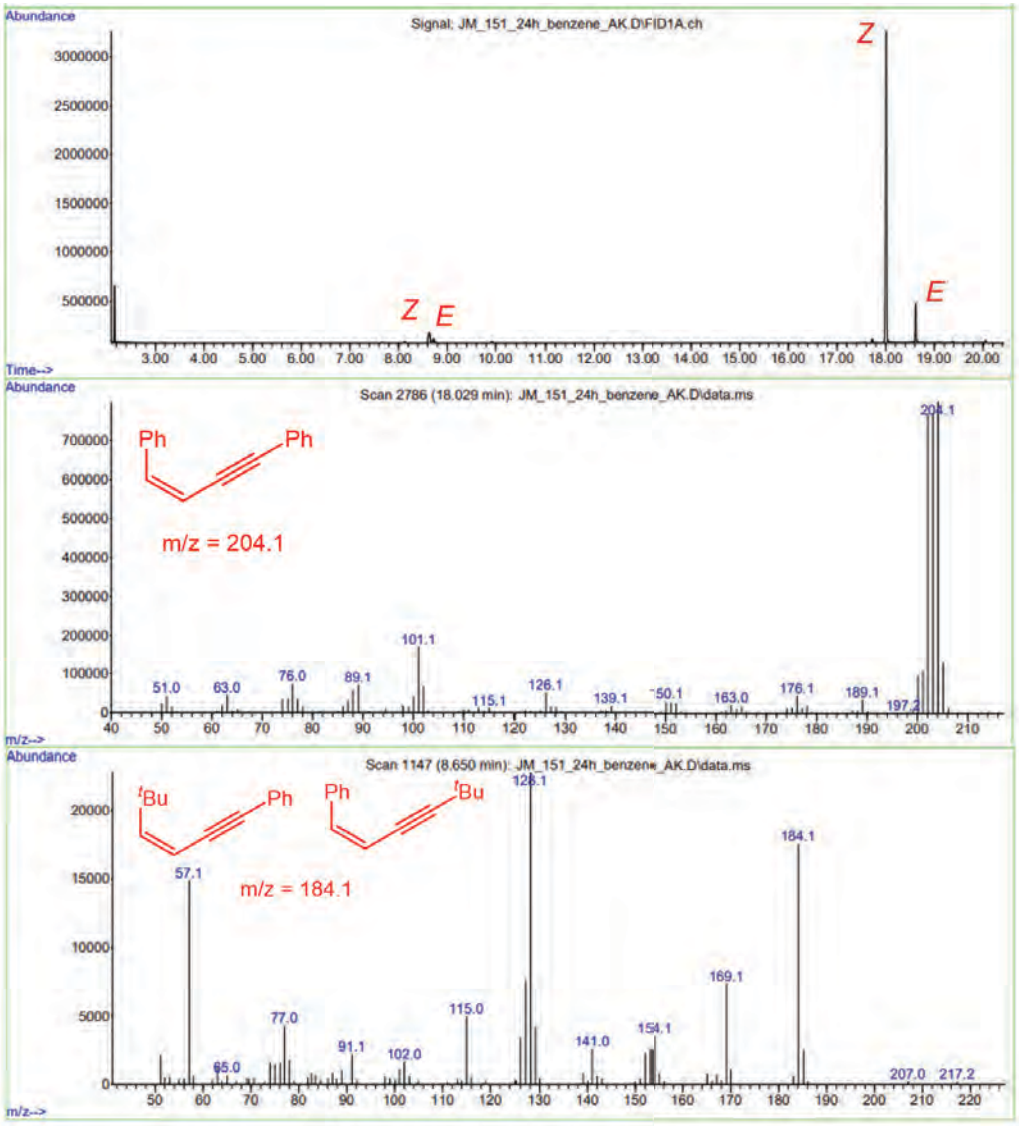

Figure S40: GC-MS chromatogram (top) and mass spectra (bottom two panels) of isolated organic products from the reaction between phenylacetylene (1 equiv) and *tert*-butyl acetylene (57 equiv) with 1 mol % 1 (C_6D_6, 30°C, 24 h).

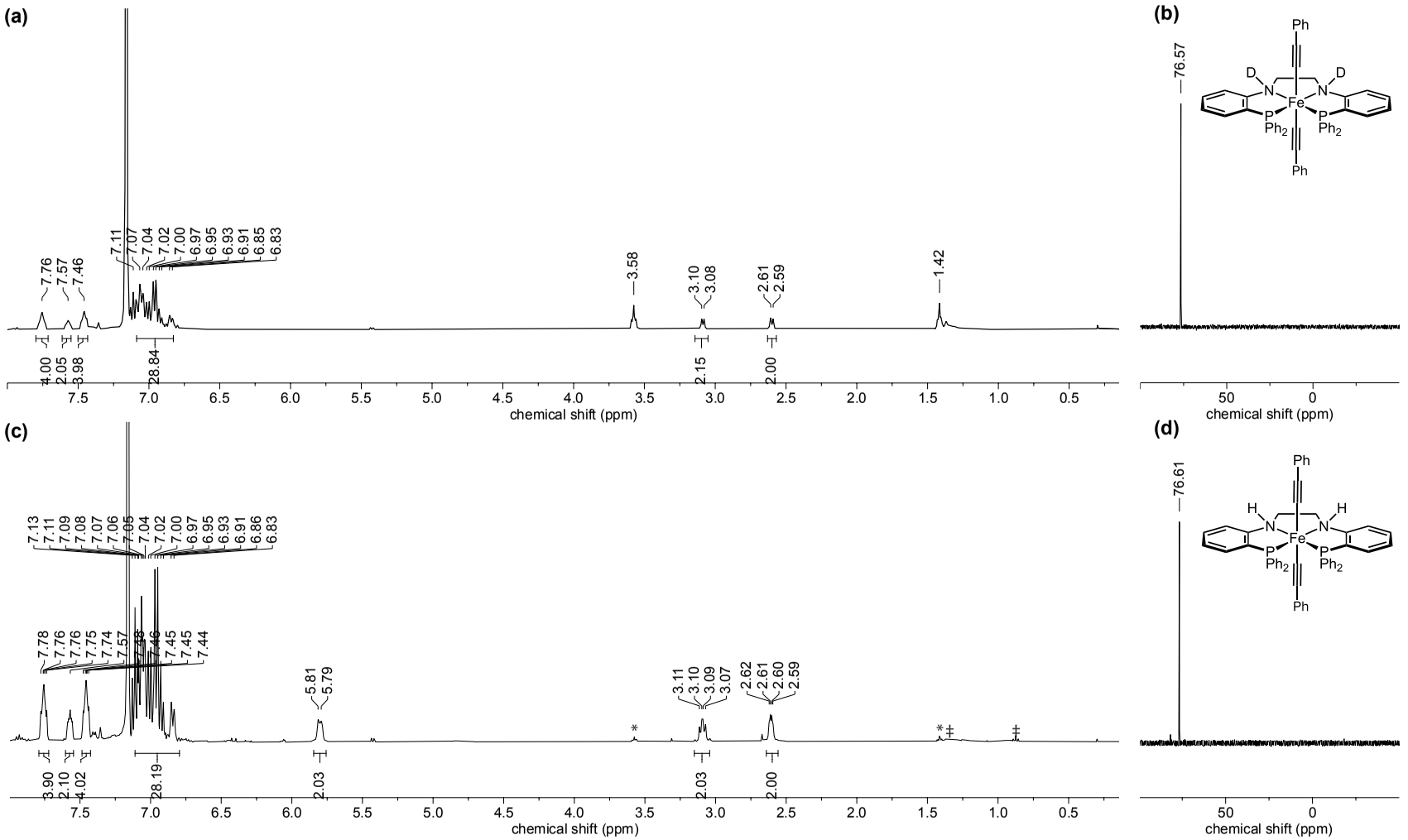

Figure S41: ^{1}H NMR spectrum (C_6D_6, 400 MHz) of **2-D** (a) and **2** (c) with $^{31}P\{^{1}H\}$ NMR spectra (C_6D_6, 162 MHz) of **2-D** (b) and **2** (d) shown to the right. Residual THF and pentane are marked with ∗ and ‡, respectively.

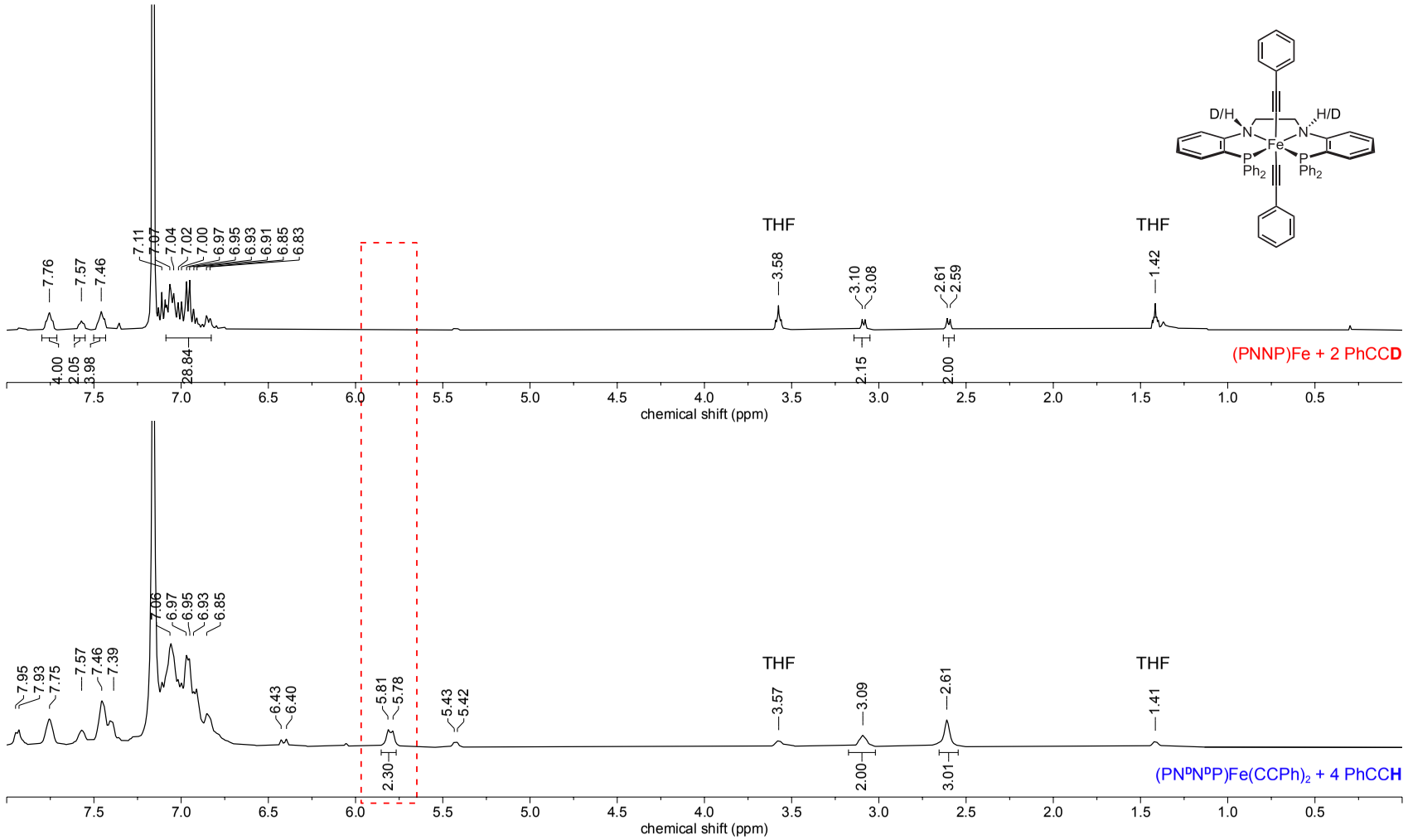

Figure S42: Stacked ^{1}H NMR spectra (C_6D_6, 400 MHz) of **2-D** before (top) and after (bottom) treatment with 4 equiv PhCCH. In the top spectrum, the characteristic N–H peak of 2 is notably absent but is restored upon treatment of **2-D** with PhCCH to give a spectrum consistent with that of **2**. In the bottom spectrum, resonances corresponding to the enyne dimer are also present, consistent with the generation of a statistical distribution of double deuterated, singly deuterated products, and non-deuterated products. Residual THF (reaction solvent) in the spectra is marked with "THF."

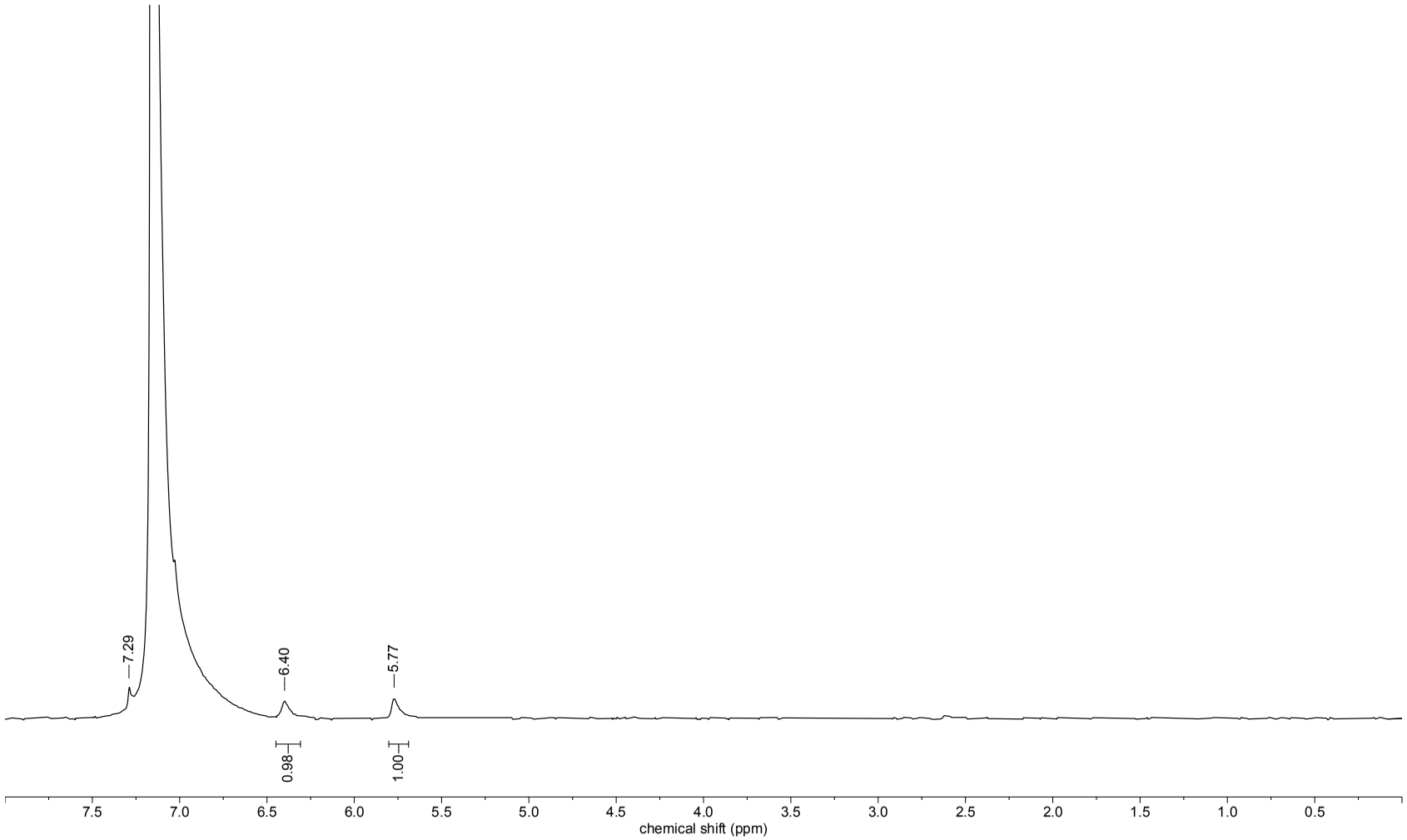

Figure S43: ^{2}H NMR (C_6H_6) of the reaction mixture of **2-D** with 4 equiv PhCCH after passage through silica to remove the leftover metal complex. A few drops of C_6D_6 were added to provide a known signal to which to reference.

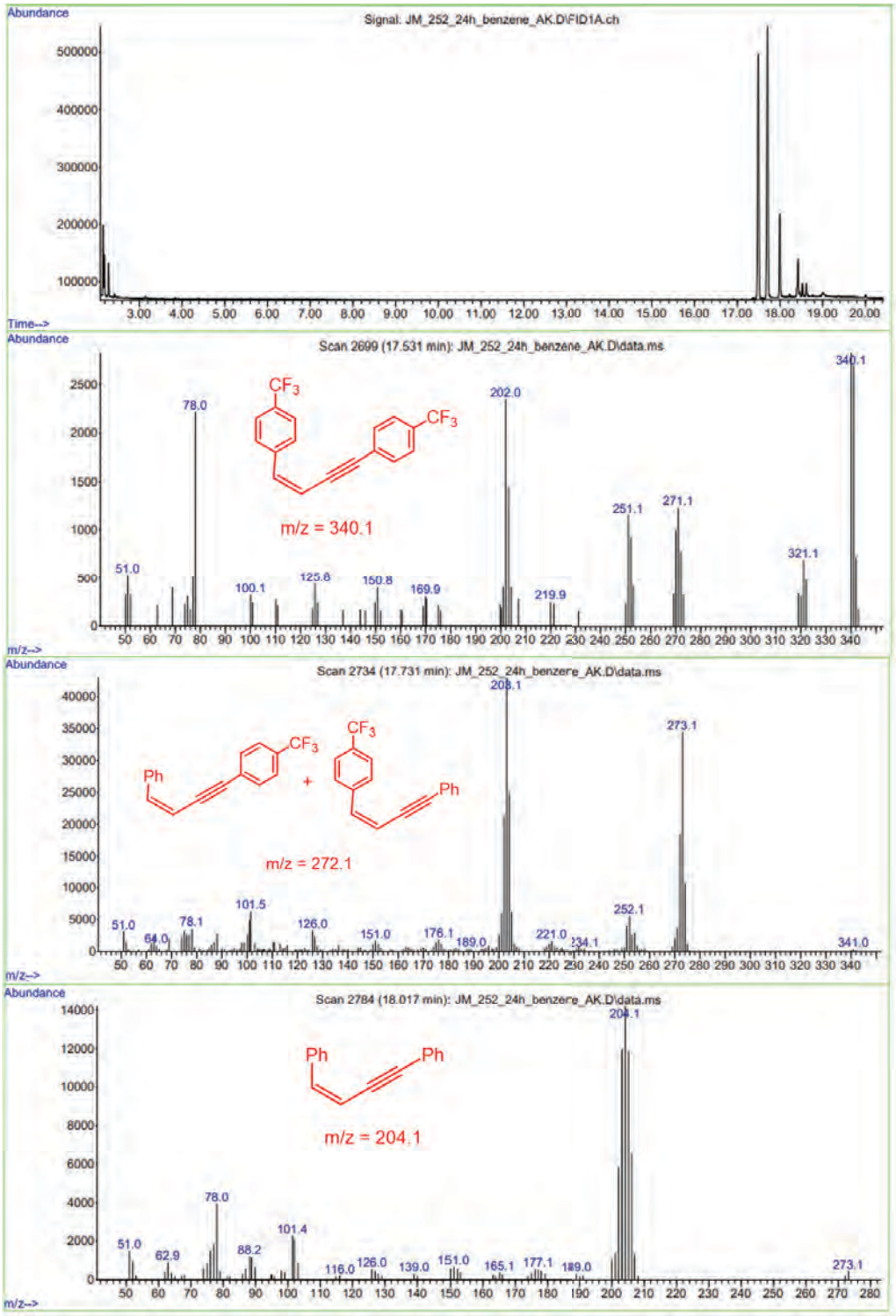

Figure S44: GC-MS chromatogram (top) and mass spectra (bottom three panels) of isolated organic products from the reaction of **2-D** with **4e**.

References

(S1) Hatzis, G. P.; Thomas, C. M. Metal–ligand cooperativity across two sites of a square planar iron(ii) complex ligated by a tetradentate PNNP ligand. *Chem. Commun.* **2020**, *56*, 8611–8614.

(S2) Garcia-Fernandez, P. D.; Iglesias-Siguenza, J.; Rivero-Jerez, P. S.; Diez, E.; Gomez-Bengoa, E.; Fernandez, R.; Lassaletta, J. M. Au(I)-Catalyzed Hydroalkynylation of Haloalkynes. *J. Am. Chem. Soc.* **2020**, *142*, 16082–16089.

(S3) Platel, R. H.; Schafer, L. L. Zirconium catalyzed alkyne dimerization for selective Z-enyne synthesis. *Chem. Commun.* **2012**, *48*, 10609–10611.

(S4) Burgio, A. L.; Buchbinder, N. W.; Santos, W. L. Regio- and Stereoselective Copper-Catalyzed Borylation-Protodeboronation of 1,3-Diynes: Access to (Z)-1,3-Enynes. *Org. Lett.* **2023**, *25*, 2652–2656.

(S5) Prisecaru, I. WMOSS-4F. 2016.

(S6) Bruker AXS, Inc. SAINT (v. 8.40b). 2021.

(S7) Bruker AXS, Inc. SADABS (v. 2016/2). 2016.

(S8) Dolomanov, O. V.; Bourhis, L. J.; Gildea, R. J.; Howard, J. A. K.; Puschmann, H. OLEX2: a complete structure solution, refinement and analysis program. *J. Appl. Crystallogr.* **2009**, *42*, 339–341.

(S9) Sheldrick, G. M. SHELXT - integrated space-group and crystal-structure determination. *Acta Crystallogr. A Found. Adv.* **2015**, *71*, 3–8.

(S10) Sheldrick, G. M. Crystal structure refinement with SHELXL. *Acta Crystallogr. C Struct. Chem.* **2015**, *71*, 3–8.

(S11) Silverstein, R. M.; Webster, F. X.; Kiemle, D. J. *Spectrometric Identification of Organic Compounds*; John Wiley and Sons, Inc.: New York, NY, 2005; Chapter Coupling of Protons to ^{31}P, p 156.